STRESS CONCENTRATION AROUND HOLES IN LAMINATED FIBROUS COMPOSITES

David Lee Saba

NAVAL POSTGRADUATE SCHOOL
Monterey, California

THESIS

STRESS CONCENTRATION AROUND HOLES IN LAMINATED FIBROUS COMPOSITES

by

David Lee Saba

June 1975

Thesis Advisor: Milton H. Bank

Prepared for:
Naval Air Systems Command
Washington, D.C. 20361

NAVAL POSTGRADUATE SCHOOL
Monterey, California

Rear Admiral I. W. Linder
Superintendent

Jack R. Borsting
Provost

This thesis prepared in conjunction with research supported in part by Naval Air Systems Command under NAIR 320B.

Released as a
Technical Report by:

UNCLASSIFIED

SECURITY CLASSIFICATION OF THIS PAGE (When Data Entered)

REPORT DOCUMENTATION PAGE

READ INSTRUCTIONS BEFORE COMPLETING FORM

1. REPORT NUMBER: NPS-57Bt75061
2. GOVT ACCESSION NO.
3. RECIPIENT'S CATALOG NUMBER

4. TITLE (and Subtitle): Stress Concentration Around Holes in Laminated Fibrous Composites

5. TYPE OF REPORT & PERIOD COVERED: Master's Thesis & June 1975 Technical Rpt

6. PERFORMING ORG. REPORT NUMBER

7. AUTHOR(s): David Lee Saba

8. CONTRACT OR GRANT NUMBER(s)

9. PERFORMING ORGANIZATION NAME AND ADDRESS: Naval Postgraduate School, Monterey, California 93940

10. PROGRAM ELEMENT, PROJECT, TASK AREA & WORK UNIT NUMBERS: 61153N; R02303-000; N00019-75-WR-51077

11. CONTROLLING OFFICE NAME AND ADDRESS: Naval Air Systems Command (NAIR-320B), Washington, D.C. 20361

12. REPORT DATE: June 1975

13. NUMBER OF PAGES

14. MONITORING AGENCY NAME & ADDRESS(if different from Controlling Office)

15. SECURITY CLASS. (of this report): Unclassified

15a. DECLASSIFICATION/DOWNGRADING SCHEDULE

16. DISTRIBUTION STATEMENT (of this Report)

Approved for public release; distribution unlimited.

17. DISTRIBUTION STATEMENT (of the abstract entered in Block 20, if different from Report)

18. SUPPLEMENTARY NOTES

19. KEY WORDS (Continue on reverse side if necessary and identify by block number)

20. ABSTRACT (Continue on reverse side if necessary and identify by block number)

The purpose of this research was to show, both experimentally and analytically, that the stress concentration around holes in laminated fibrous composites is not adequately described by the theoretical solution for homogeneous orthotropic plates, and that it is a function of hole size. It was shown that the gross laminate properties, determined analytically from individual lamina properties, make it impossible to express the proper

DD FORM 1 JAN 73 1473 EDITION OF 1 NOV 65 IS OBSOLETE
S/N 0102-014-6601

UNCLASSIFIED

SECURITY CLASSIFICATION OF THIS PAGE (When Data Entered)

boundary conditions at a free edge. A new expression for the modulus of elasticity tangential to a free boundary was developed. Thus, the problem became similar to that of a circular hole strengthened by an elastic ring. Furthermore, the effective width of such a ring was found to depend upon hole size. Thus, the stress concentration factor was shown to be a function of hole size, which was not predicted by homogeneous orthotropic theory. These results were very satisfactorily verified by experiment.

Stress Concentration Around Holes in Laminated Fibrous Composites

by

David Lee Saba
Ensign, United States Navy
B.S., United States Naval Academy, 1974

Submitted in partial fulfillment of the
requirements for the degree of

MASTER OF SCIENCE IN AERONAUTICAL ENGINEERING

from the

NAVAL POSTGRADUATE SCHOOL
June 1975

ABSTRACT

The purpose of this research was to show, both experimentally and analytically, that the stress concentration around holes in laminated fibrous composites is not adequately described by the theoretical solution for homogeneous orthotropic plates, and that it is a function of hole size. It was shown that the gross laminate properties, determined analytically from individual lamina properties, make it impossible to express the proper boundary conditions at a free edge. A new expression for the modulus of elasticity tangential to a free boundary was developed. Thus, the problem became similar to that of a circular hole strengthened by an elastic ring. Furthermore, the effective width of such a ring was found to depend upon hole size. Thus, the stress concentration factor was shown to be a function of hole size, which was not predicted by homogeneous orthotropic theory. These results were very satisfactorily verified by experiment.

TABLE OF CONTENTS

LIST OF FIGURES

LIST OF TABLES

LIST OF SYMBOLS

G	-	shear modulus
G/E	-	glass/epoxy
E	-	modulus of elasticity
K	-	strain concentration
n	-	material parameter given by eqn (II.E.2)
X	-	transverse distance from center of hole (II.E.1)
Y	-	longitudinal distance from center of hole (II.E.1)
[C]	-	stiffness matrix
$[\bar{C}]$	-	transformed stiffness matrix
[T]	-	transformation matrix (Eqn III.A.3)
ε	-	strain
σ	-	stress
ν	-	Poisson's ratio
τ	-	shear stress
γ	-	shear strain
α	-	lamina orientation angle from longitudinal axis
θ	-	angle from longitudinal axis
P	-	load
h	-	thickness

SUBSCRIPTS

1	-	longitudinal axis of composite plate
2	-	transverse axis of composite plate
45	-	45° between 1 and 2 directions
ℓ	-	longitudinal (fiber) axis of a lamina

t - transverse axis of a lamina

n - normal to plate boundary

s - tangential to plate boundary

θ - arbitrary angle from longitudinal axis

SUPERSCRIPTS

c - composite plate (includes photoelastic coating)

c-P - composite plate less photoelastic coating

P - photoelastic coating

(k) - denotes K^{th} lamina

I. INTRODUCTION

A. BACKGROUND

Because of their high strength-to-weight ratios, laminated fibrous composites are expected to be utilized extensively for aerospace vehicles in the future. At the present time, however, the realization of the maximum potential of composites is severely restricted by the limited techniques available for their analysis. An aerospace vehicle is necessarily a very complex structure which is difficult to analyze even when composed of homogeneous isotropic materials. The introduction of inhomogeneous anisotropic composites greatly magnifies the problem. Lekhnitskii presents a solution for stresses around elliptic holes in homogeneous orthotropic plates, but the applicability to nonhomogeneous composites is questionable.

B. OBJECTIVES

The first objective of this research was to show experimentally that the homogeneous orthotropic solution for stress concentration around a circular hole is not accurate for laminated fibrous composites. The second objective was to determine whether hole size has an effect on the stress concentration in an infinite plate. The third objective was to analyze the effects of inhomogeneity on stress concentration. Specifically, the boundary conditions on a free edge in an inhomogeneous laminate were analyzed in general and

in particular for the composite tested experimentally in this research.

C. APPROACH

As stated above, the experimental objectives required the comparison of stress fields for different hole sizes with the homogeneous orthotropic solution. A $(0°, \pm 45°)_s$ glass-epoxy composite was used. Four different hole sizes were tested by reflection photoelasticity. The analytical approach was to examine the relationships between constituent, lamina, and laminate material properties given by Calcote[2]. The purpose of this analysis was to determine if this attempt to represent laminated fibrous composites as homogeneous materials was valid near free boundaries.

II. EXPERIMENTAL ANALYSIS

A. SPECIMEN DESIGN

1. Material Properties

The solution given by Lekhnitskii [3] for the stress concentration around a circular hole in an orthotropic plate is dependent upon the material properties. Therefore, the first task was to determine these properties experimentally. Due to the thickness of the photoelastic coating to be used for the stress concentration analysis, the entire glass-epoxy-photoelastic system was analyzed as a whole, rather than trying to apply correction factors. Thus, the material properties were also obtained by photoelasticity.

Determination of the material properties of an orthotropic material requires tension specimens cut along the principle l-t axes, and a third specimen cut at 45° to these axes[2]. Therefore, standard tensile specimens as described in the Advanced Composites Design Guide [1] were made up.

2. Stress Concentration

Previous experimental work by this author seemed to indicate that stress concentration in composites is a function of hole size. One purpose of the present research was to attempt to verify this hypothesis. Therefore, hole size was the only independent variable considered in designing specimens. All specimens were cut from the same sheet of material. The width of each specimen was twelve times the

hole radius. The dimensions of all specimens are given in Table II.A.1.

TABLE II.A.1

1200 SERIES SPECIMENS

MATERIAL: GLASS/EPOXY/PS1-C

G/E LAYUP: $(0°, \pm 45°)_S$

THICKNESS: .15"

PLATE #	LENGTH L (in)	WIDTH W (in)	HOLE DIAMETER (2a)	STRESS ANGLE (α)
1200	9	1	-	0°
1210	9	1	-	45°
1220	9	1	-	90°
1203	18	3	1/2	0°
1205	12	1-1/2	1/4	0°
1206	7-1/2	3/4	1/8	0°

B. SPECIMEN PREPARATION

The G/E composite was obtained from 3-M Company in a two by three foot sheet. The specimens were cut from this sheet using a diamond edge saw. All cutting operations were water cooled. The ends of each specimen were built up by attaching pieces of (0°, 90°) G/E as described in the Composites Design

Guide. The most difficult operation was that of drilling holes in the G/E material. The difficulty lay in preventing fiber pullout as the drill bit came out the back of the material. This problem was overcome by sandwiching the composite between aluminum when drilling.

The PS-1C photoelastic coating was cut one-eighth inch oversize and the holes were drilled. After cementing the coating to both sides of the G/E composite, the holes were reamed and the edges were trimmed by machining at high speed.

C. TESTING PROCEDURE

The photoelastic data was taken using the 030 series reflection polariscope by Photolastic, Inc. The specimens were mounted in a Reihle 10,000 lb. testing machine. In order to reduce the scatter due to viscoelastic effects, specimens 1200, 1210, and 1220 were cycled to 300 lb. three times before testing began. The other specimens were held at their test load for five minutes before taking data. The tare values were taken after this initial stretching.

D. MATERIAL PROPERTIES RESULTS

The original and reduced data are given in tabular form in the Appendix. Note that the fringe value, F, has been divided by the scale factor of 47 of the linear compensator. Thus, the "fringe orders" given (i.e. NN, NO, TNN, and TNO) are actually compensator readings. Using these data, the stress-strain curves for each specimen and the Poisson's Ratio vs. strain curves for specimens 1200 and 1220 were

point plotted (Figures II.D.1-5). There is considerable data scatter, particularly in Poisson's Ratio. Although a good deal of effort was directed towards eliminating this scatter, viscoelastic effects and slight variations in load during testing made the task extremely difficult. It appears that the viscoelastic properties of the material affect the transverse strain to an even greater degree than the longitudinal strain. In view of these difficulties, due consideration was given to the relationship,

$$E_1 \nu_{21} = E_2 \nu_{12} \qquad \text{(II.D.1)}$$

when the curves were drawn in these figures. Using the equation

$$\frac{1}{G_{12}} = \frac{4}{E_{45}} - \frac{1}{E_1} - \frac{1}{E_2} + \frac{2\nu_{12}}{E_1} \qquad \text{(II.D.2)}$$

the following material properties were derived from the curves:

$$E_1^c = 1.24 \text{ MSI} \qquad \nu_{12} = .5$$

$$E_2^c = 0.78 \text{ MSI} \qquad \nu_{21} = .31$$

$$G_{12} = .51 \text{ MSI}$$

E. STRESS CONCENTRATION RESULTS

A point-by-point photoelastic analysis was done for plates 1203, 1205, and 1206. The points chosen were along the X and

FIGURE II.D.1. - LONGITUDINAL MODULUS

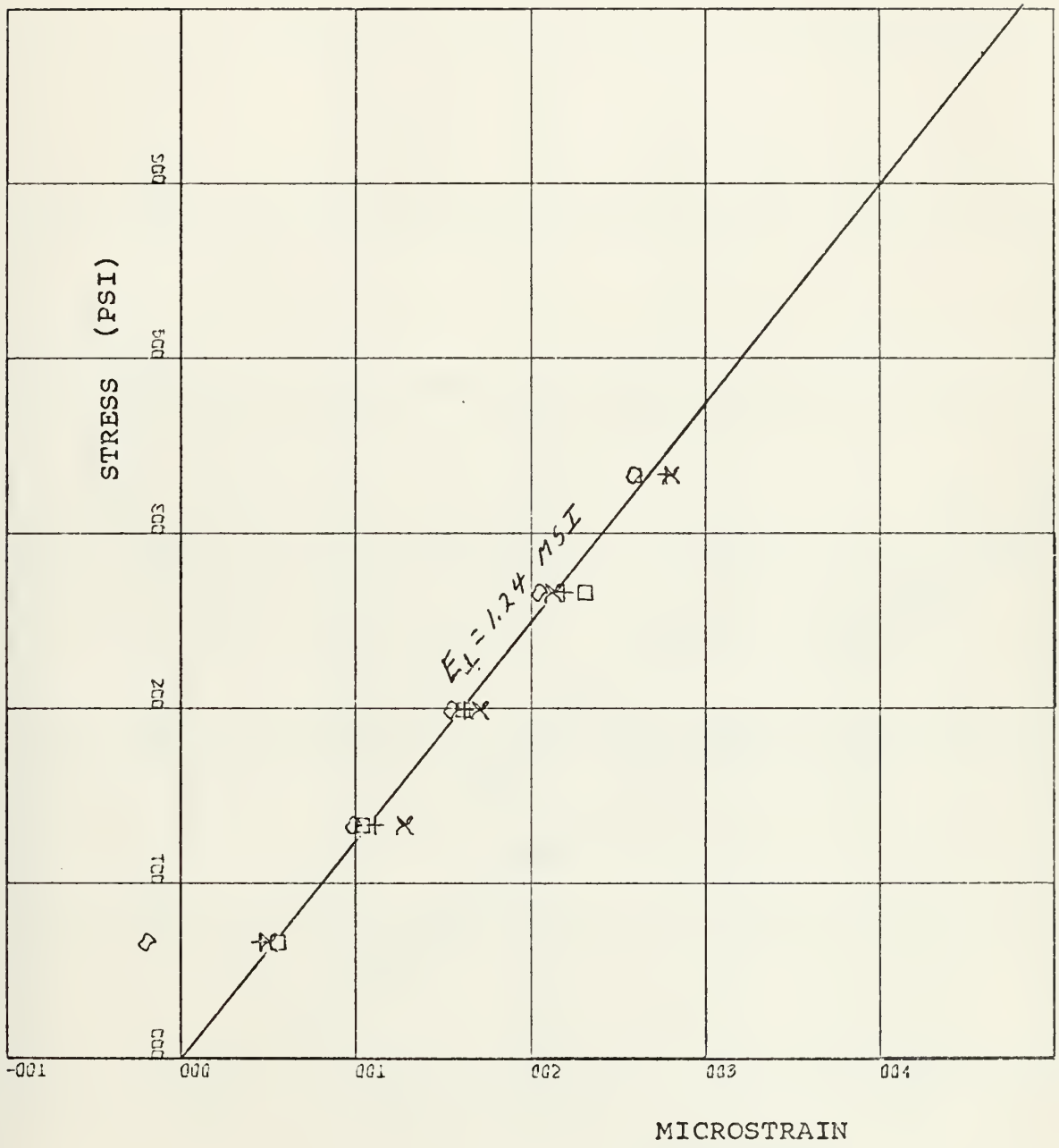

X-SCALE=1.00E+03 UNITS INCH.
Y-SCALE=1.00E+03 UNITS INCH.
PLATE # 1200

FIGURE II.D.2 - Modulus at 45 Degrees

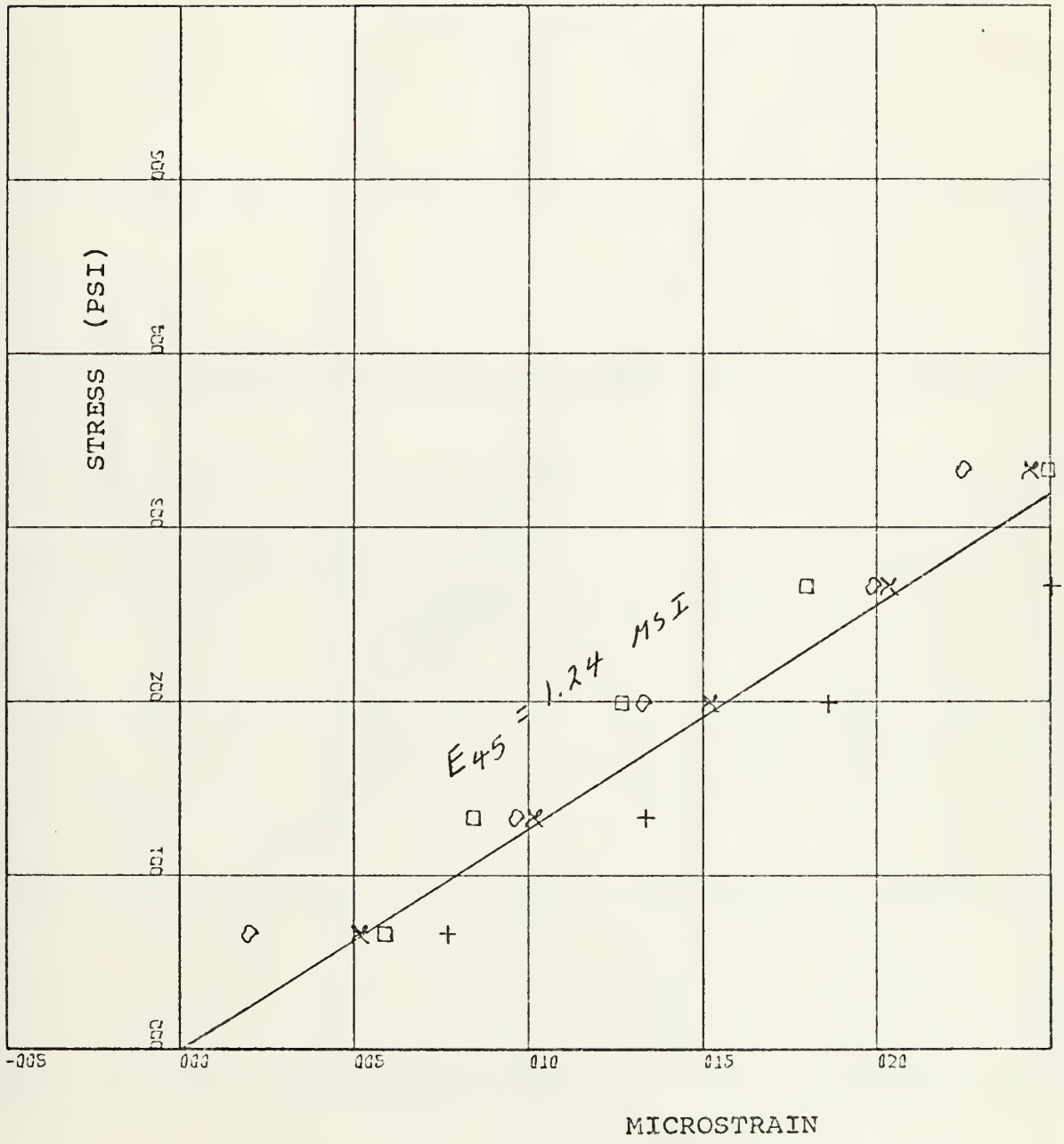

X-SCALE=5.00E+02 UNITS INCH.
Y-SCALE=1.00E+03 UNITS INCH.
PLATE # 1210

FIGURE II.D.3 - TRANSVERSE MODULUS

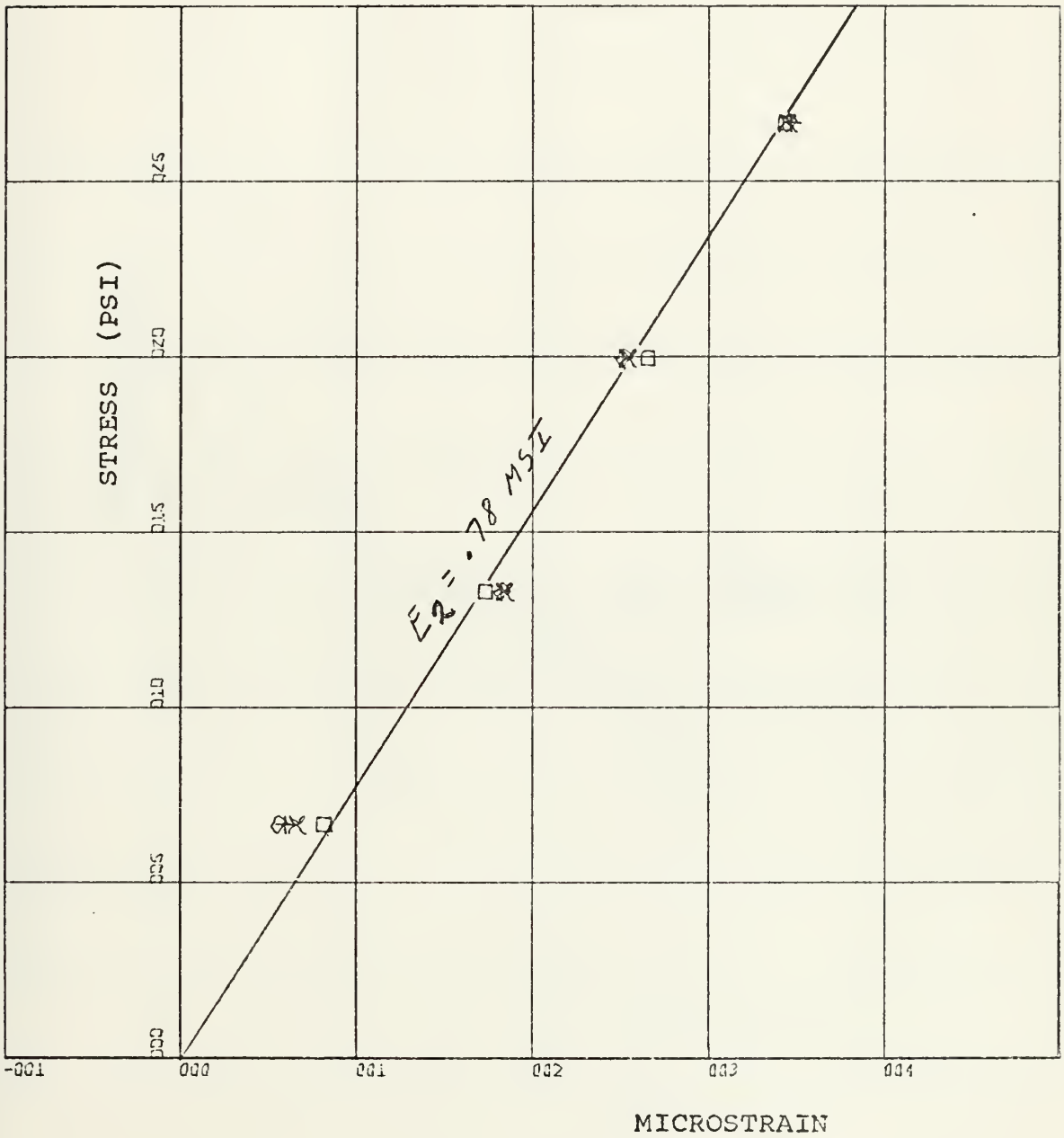

X-SCALE=1.00E+03 UNITS INCH.
Y-SCALE=5.00E+02 UNITS INCH.
PLATE # 1220

FIGURE II.D.4 - Longitudinal Poisson's Ratio

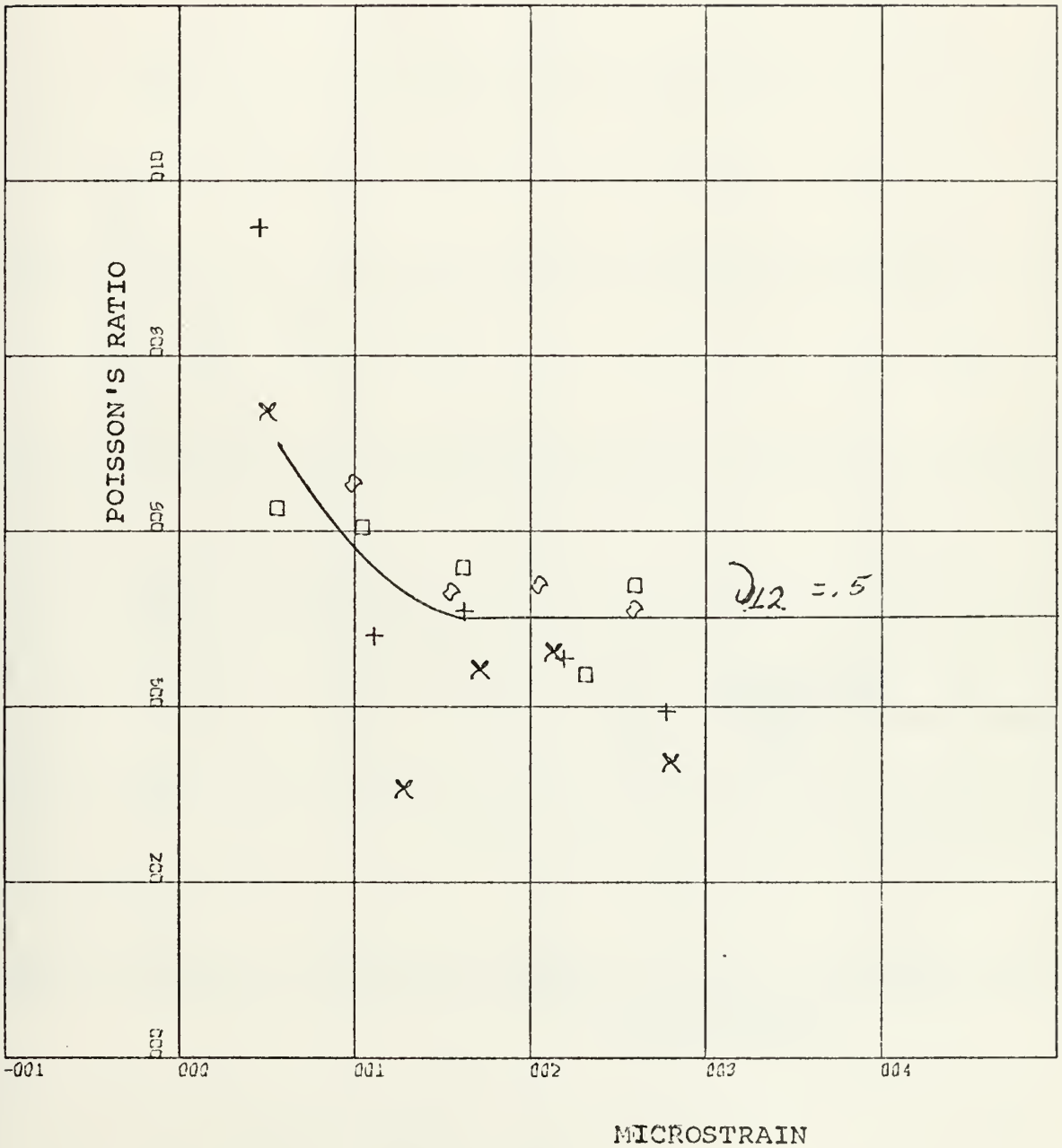

X-SCALE=1.00E+03 UNITS INCH.
Y-SCALE=2.00E-01 UNITS INCH.
PLATE # 1200

FIGURE II.D.5 - Transverse Poisson's Ratio

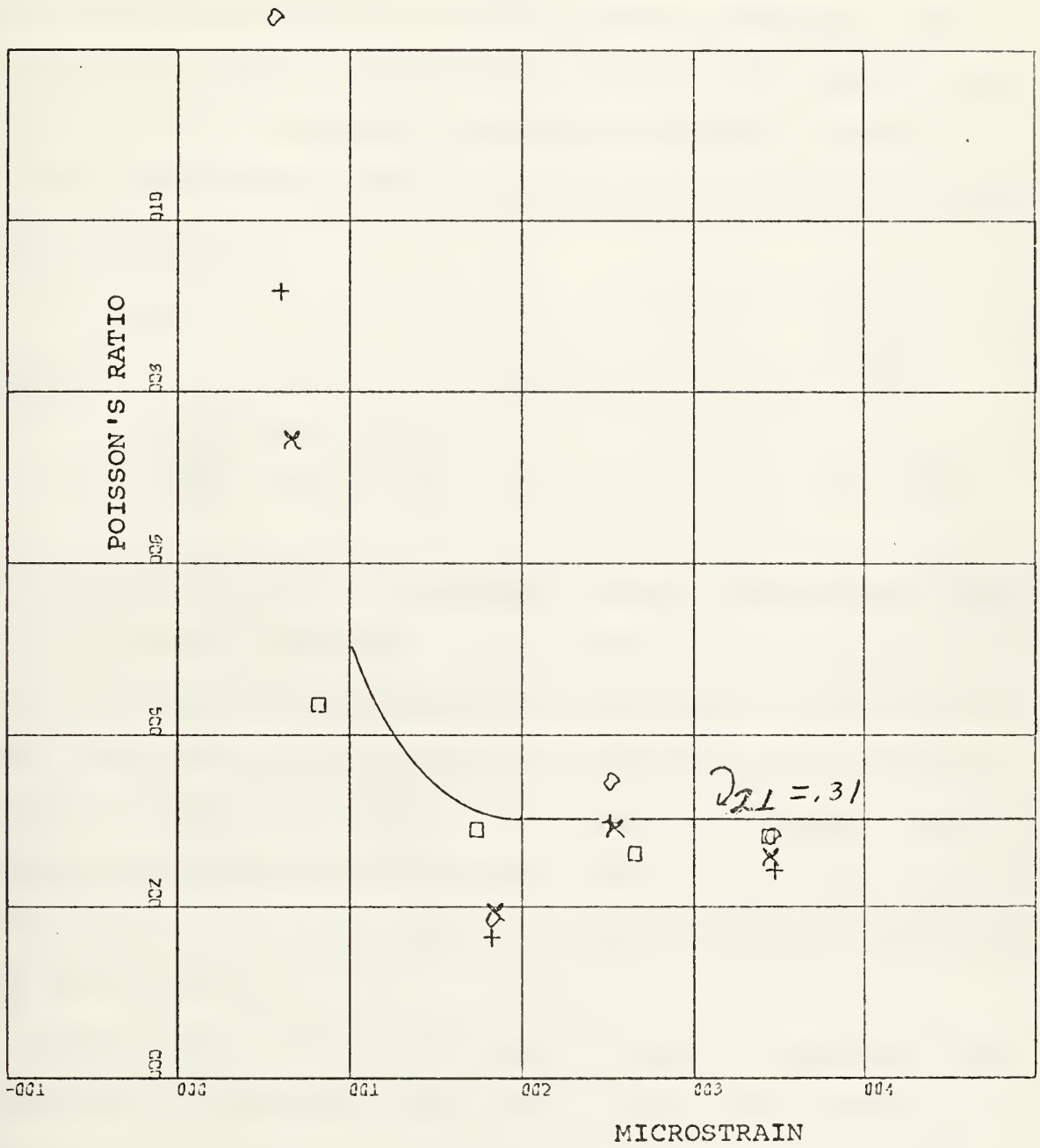

X-SCALE=1.00E+03 UNITS INCH.
Y-SCALE=2.00E-01 UNITS INCH.
PLATE # 1220

Y axes as shown in Figure II.E.1. The data are tabulated in the Appendix as explained in the previous paragraph. The longitudinal strain variation along the X-axis from the hole to the edge of the plate is plotted in Figures II.E.2-5.

The theoretical strain concentration at the hole is given by Lekhnitskii as

$$K = p(1+n) \qquad \text{(II.E.1)}$$

where

$$n = \sqrt{2\left(\frac{E_1}{E_2} - \nu_{12}\right) + \frac{E_1}{G_{12}}} \qquad \text{(II.E.2)}$$

These equations give a theoretical strain concentration factor of 3.15 for this material. It is evident from Figure II.D.5 that the strain concentration is a function of hole size for this laminated fibrous composite, even though the hole-size-to-plate-width ratio is the same. Also, the measured value seems to approach the theoretical value as hole size increases. Previous tests by this author on plates of constant width gave the same results.

Figure II.D.5 also shows that the higher the strain concentration <u>at</u> the hole, the faster it drops off with the <u>normalized</u> distance from the hole. In fact, the former is actually <u>lower</u> at some points! This phenomenon is necessary so that the average value of the stress concentration over the entire X-axis (including the hole) will be equal to one. Note also the drop in strain concentration at the outside edge

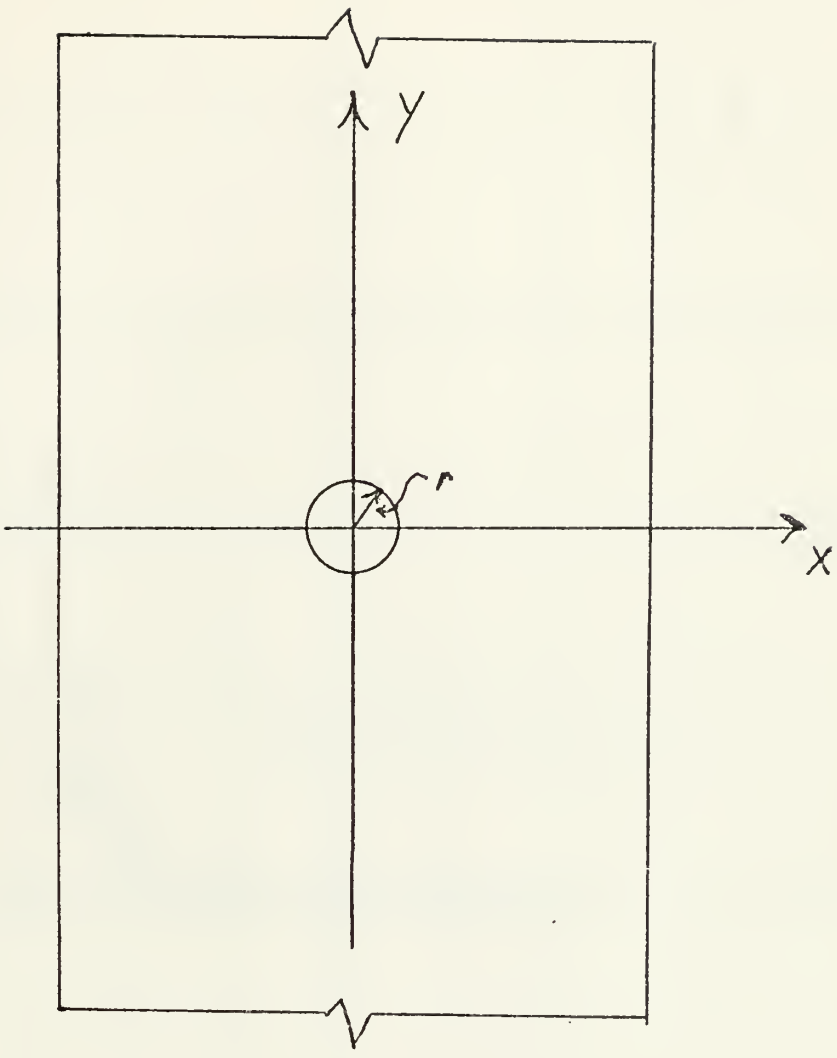

FIGURE II.E.1 - Coordinate System

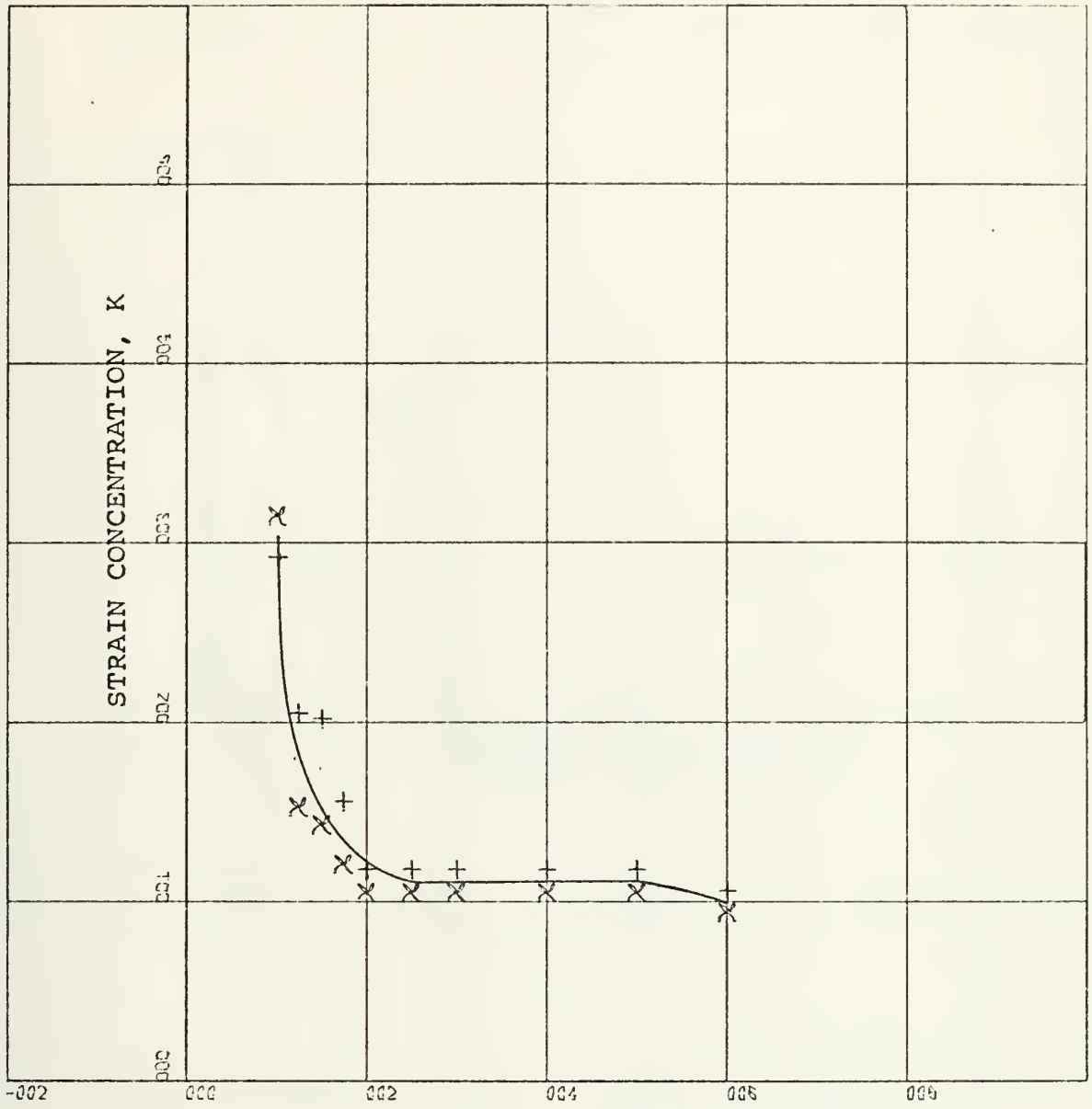

X-SCALE=2.00E+00 UNITS INCH.
Y-SCALE=1.00E+00 UNITS INCH.
PLATE # 1203 X-AXIS

FIGURE II.E.2 - Strain Concentration

SABA0072

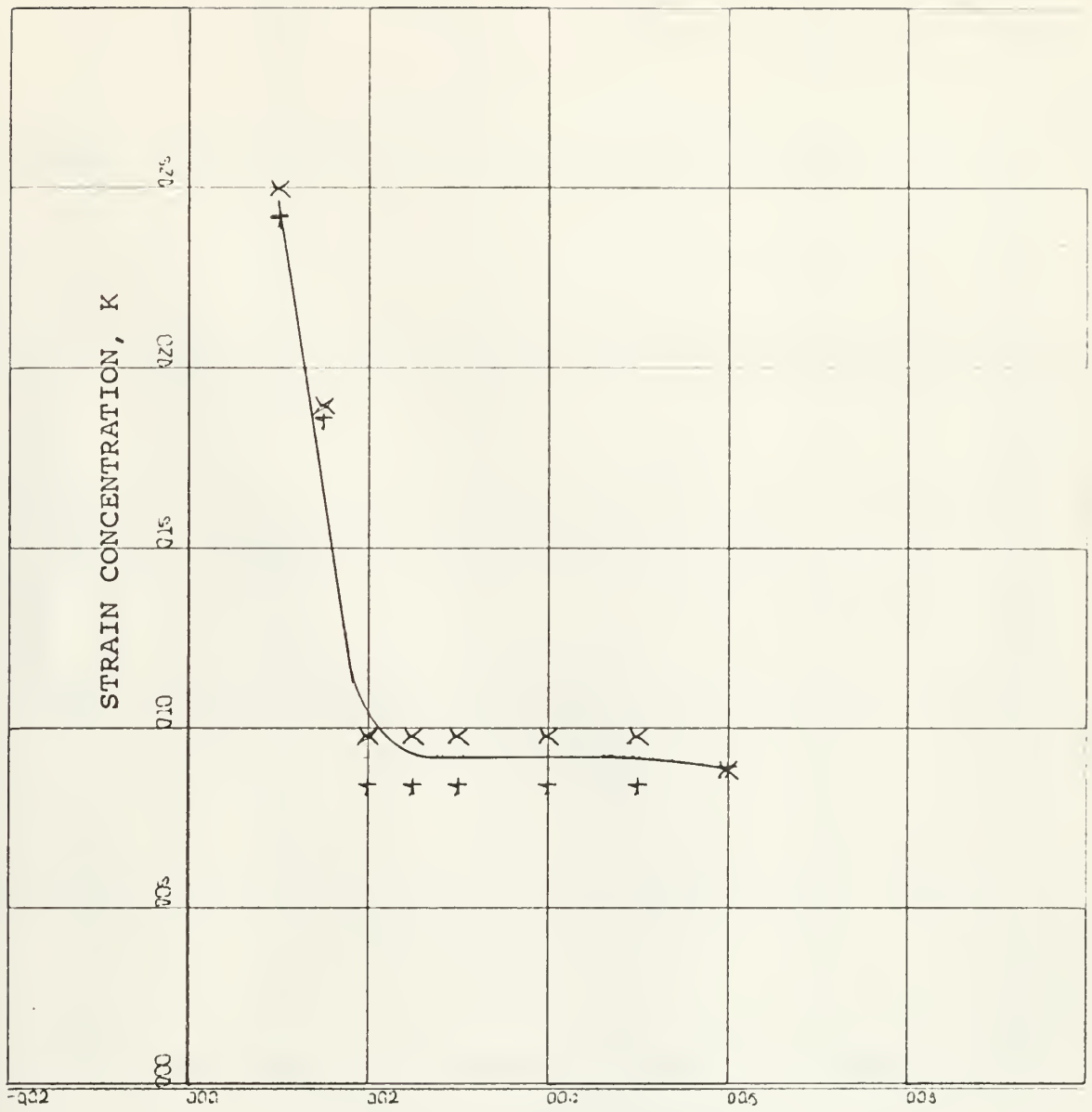

FIGURE II.E.3 - Strain Concentration

SABA0072

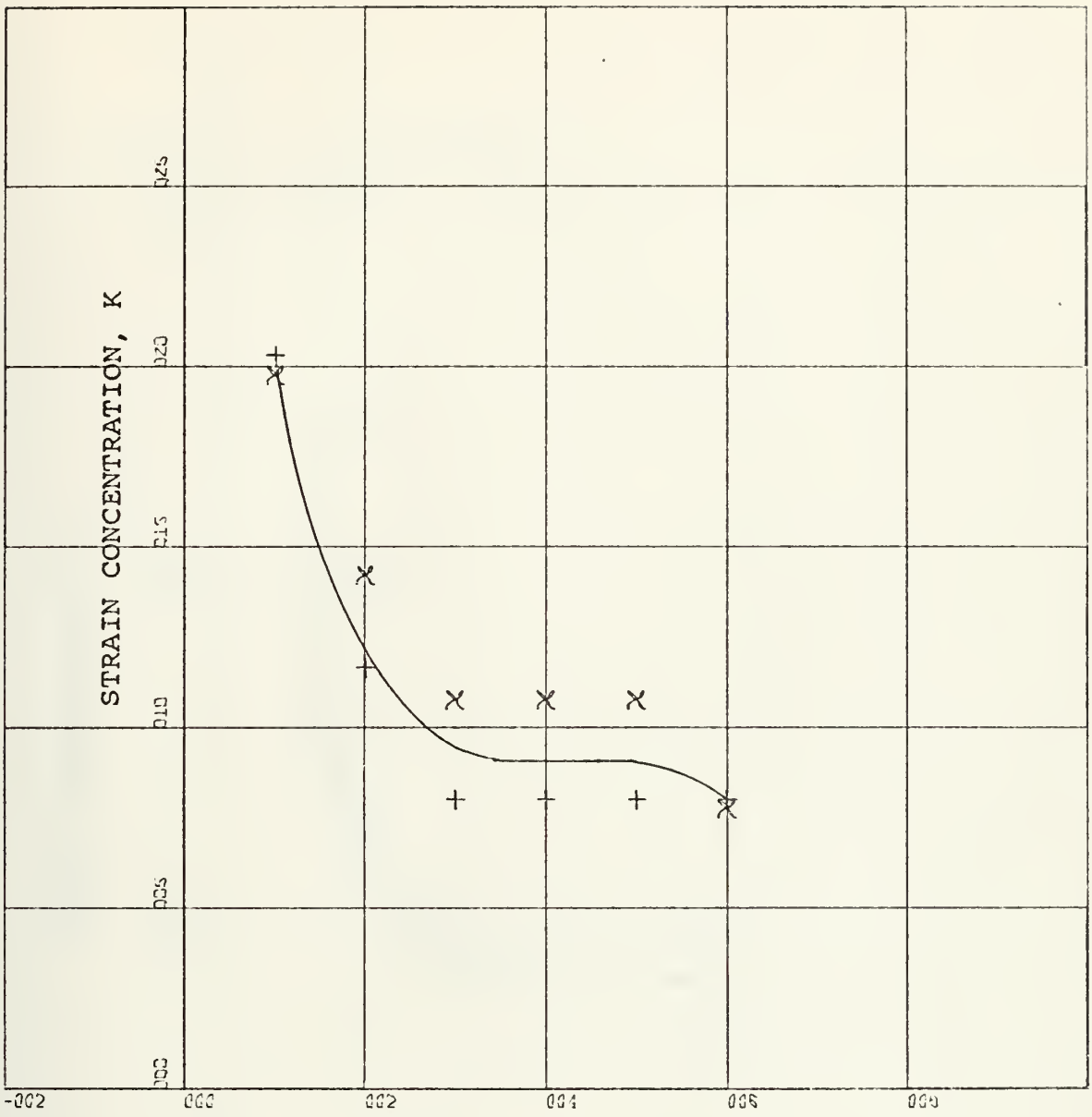

FIGURE II.E.4 - STRAIN CONCENTRATION

SABA0072

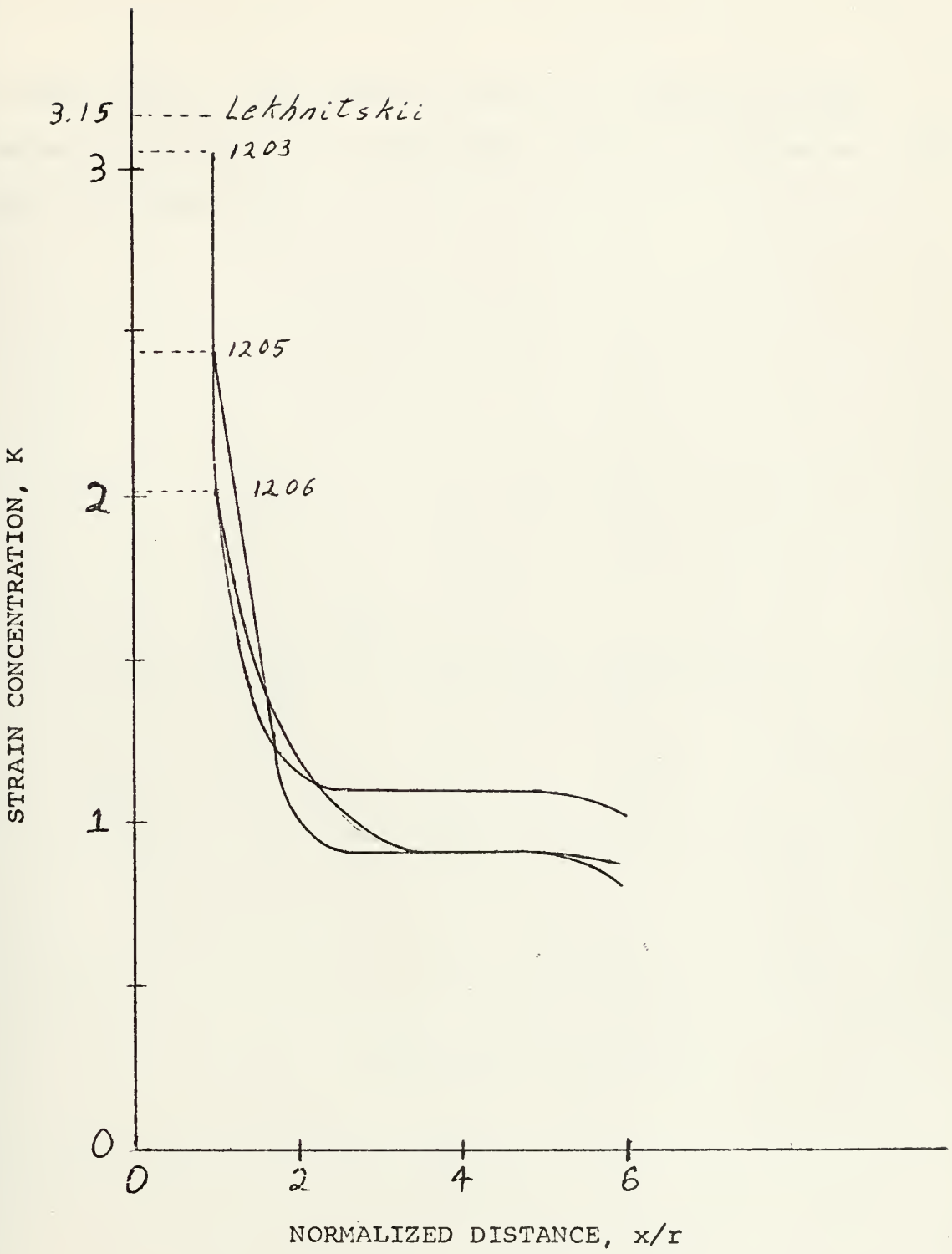

FIGURE II.E.5 - Strain Concentration

of each plate. This effect is due to a change in gross laminate properties at a free edge, which is discussed in detail in Section III.

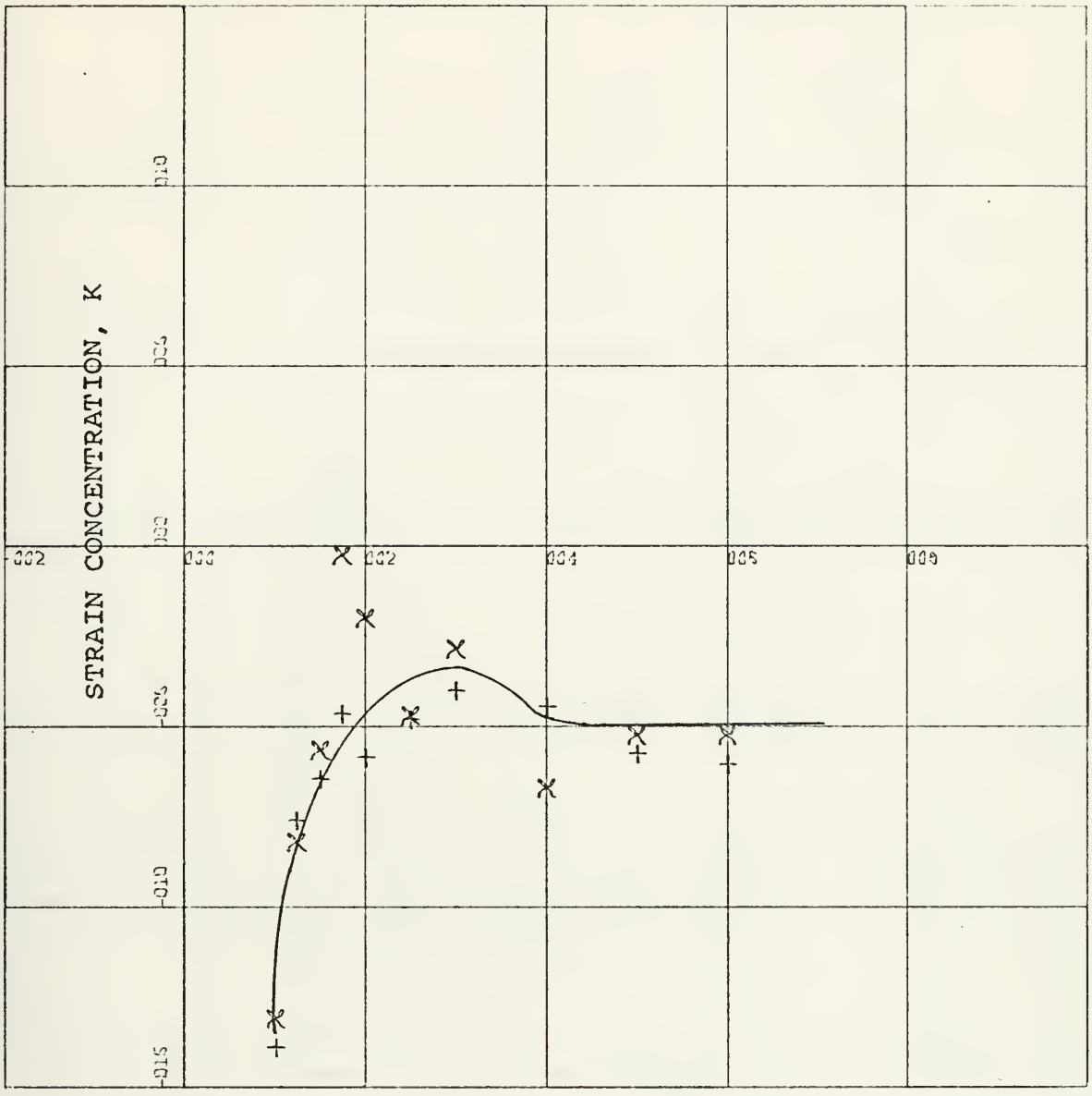

FIGURE II.E.6 - Strain Concentration

SABA0072

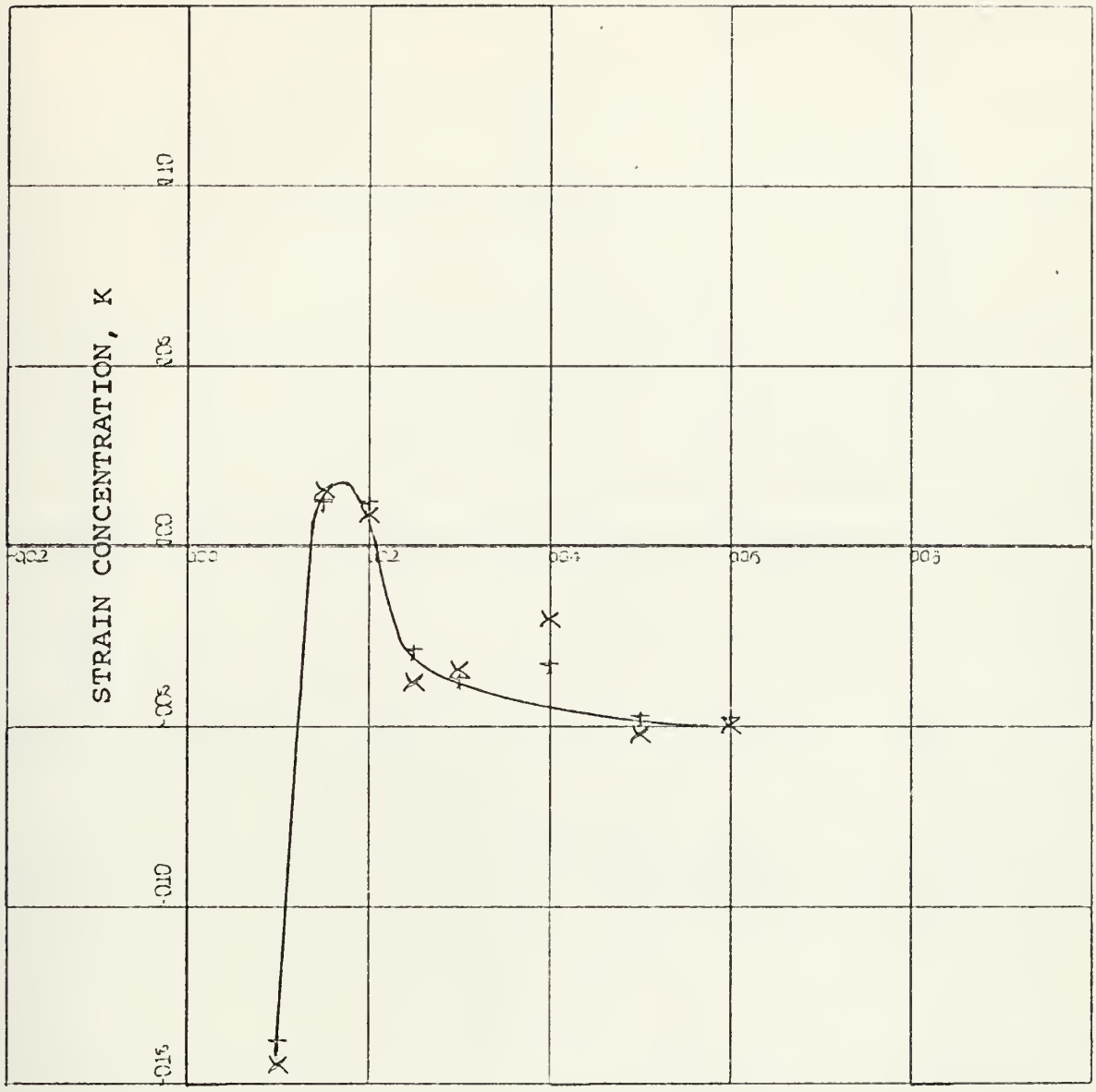

FIGURE II.E.7 - Strain Concentration

SABA0072

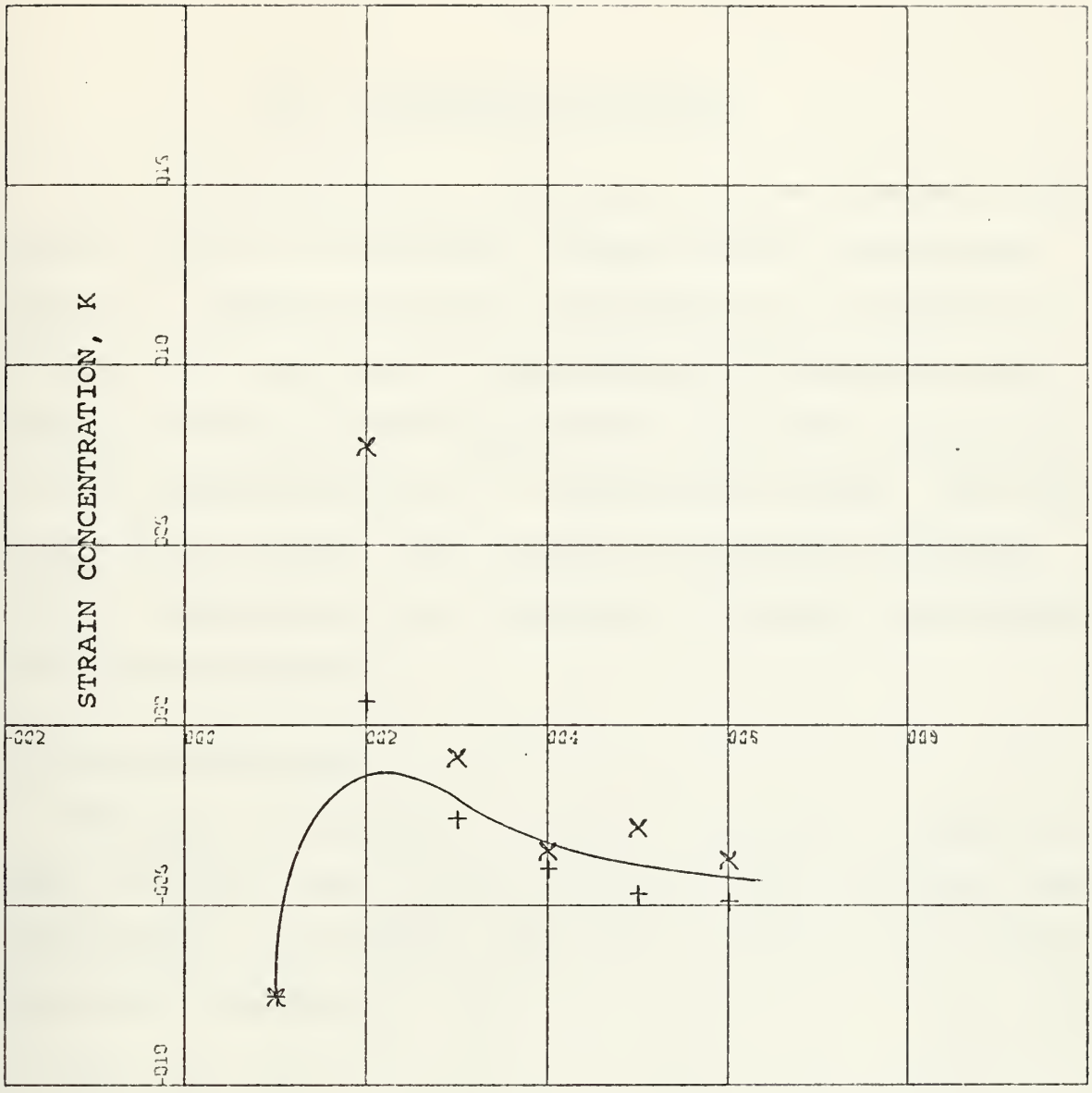

FIGURE II.E.8 - Strain Concentration

SABA0072

III. THEORETICAL ANALYSIS

The solution given by Lekhnitskii for the stresses around elliptic holes in orthotropic plates assumes a homogeneous material. Because the stress distribution is a function of the material properties, it is necessary to formulate gross laminate properties which approximate the elastic properties of the composite by those of a homogeneous system. The obvious question here is, "Are the basic assumptions necessary for this formulation valid throughout the plate, particularly near a free boundary?"

A. BASIC FORMULATION

The basic formulation will first be derived in detail because it is the basis for the discussion which follows. The stress-strain relationship (referred to natural axes) for an orthotropic lamina is

$$\{\sigma\} = [C]\ \{\varepsilon\} \qquad \text{(III.A.1)}$$

where

$$\{\sigma\} = \begin{Bmatrix} \sigma_\ell \\ \sigma_t \\ \tau_{\ell t} \end{Bmatrix}$$

$$\{\varepsilon\} = \begin{Bmatrix} \varepsilon_\ell \\ \varepsilon_t \\ 1/2\gamma_{\ell t} \end{Bmatrix}$$

and

$$[C] = \begin{bmatrix} C_{11} & C_{12} & 0 \\ C_{12} & C_{22} & 0 \\ 0 & 0 & C_{44} \end{bmatrix}$$

Referred to arbitrary axes, this relationship becomes [2]

$$\begin{Bmatrix} \sigma_1 \\ \sigma_2 \\ \tau_{12} \end{Bmatrix} = [\bar{C}] \begin{Bmatrix} \varepsilon_1 \\ \varepsilon_2 \\ 1/2\tau_{12} \end{Bmatrix} \qquad \text{(III.A.2)}$$

where

$$[\bar{C}] = [T]^{-1} [C] [T]$$

and [T] is the matrix of direction cosines:

$$[T] = \begin{bmatrix} \cos^2\alpha & \sin^2\alpha & 2\sin\alpha & \cos\alpha \\ \sin^2\alpha & \cos^2\alpha & -2\sin\alpha & \cos\alpha \\ -\sin\alpha\cos\alpha & \sin\alpha\cos\alpha & \cos^2\alpha & -\sin^2\alpha \end{bmatrix} \qquad \text{(III.A.3)}$$

Equilibrium requires that (assuming unit width)

$$\{P\}^c = \Sigma\{P\}^{(k)} = \Sigma[\sigma]^{(k)} h^{(k)}$$

where $h^{(k)}$ is the thickness of the k^{th} lamina. Thus,

$$\{\sigma\}^c = \frac{\Sigma\{\sigma\}^{(k)} h^{(k)}}{\Sigma h^{(k)}} \qquad \text{(III.A.4)}$$

Substituting equation III.A.2 into this expression yields

$$[C]^c\{\varepsilon\}^c = \frac{\Sigma[\bar{C}]^{(k)}\{\varepsilon\}^{(k)} h^{(k)}}{\Sigma h^{(k)}} \qquad \text{(III.A.5)}$$

At this point, the assumption is made that the strain field in each lamina is identical to that of the composite as a whole, that is

$$\{\varepsilon\} = \{\varepsilon\}^c = \{\varepsilon\}^{(k)} \qquad \text{(III.A.6)}$$

equals a constant over the summation. Thus, equation III.A.5 reduces to

$$[C]^c = \frac{\Sigma[\bar{C}]^{(k)} h^{(k)}}{\Sigma h^{(k)}} \qquad \text{(III.A.7)}$$

B. FREE EDGE BOUNDARY CONDITIONS

The boundary condition for a free edge in a homogeneous plate loaded in-plane is

$$\sigma_n = 0 \qquad \text{(III.B.1)}$$

By applying this boundary condition to a composite represented by the homogeneous properties given by III.A.7, one is actually only requiring that the <u>average</u> stress across the thickness be zero, rather than the stress at <u>each point</u> across the thickness of the plate. Applying equation III.A.4 to III.B.1,

$$\sigma_n^c = \frac{\Sigma\sigma_n^{(k)} h^{(k)}}{\Sigma h^{(k)}} = 0 \qquad \text{(III.B.2)}$$

Thus, $\sigma_n^{(k)}$ in general need not be zero, whereas the physics of the problem require that it must be zero. Therefore, the material properties given by equation III.A.7 are not valid near a free boundary in a laminated composite.

Equation III.B.2 results in the free-edge displacement shown in Figure III.B.2. The free edge is still a plane normal to the surface. Thus, all strains and displacements are constant through the thickness. The stress $\sigma_n^{(k)}$ in a lamina is derived as follows. The tangential stress, σ_s^c, is known and the normal stress, σ_n^c, is zero. Thus, at the free edge

$$\varepsilon_s^{(k)} = \varepsilon_s^c = \sigma_s^c / E_s^c \qquad \text{(III.B.3)}$$

and

$$\varepsilon_n^{(k)} = \varepsilon_n^c = -\nu_{sn}^c \varepsilon_s^c$$

But

$$\sigma_n^{(k)} = \left(\frac{E_n}{1-\nu_{ns}\nu_{sn}}\right)^{(k)} \left(\varepsilon_n^c + \nu_{sn}^{(k)} \varepsilon_s^c\right)$$

or

$$\sigma_n^{(k)} = \left(\frac{E_n}{1-\nu_{ns}\nu_{sn}}\right)^{(k)} \left(\nu_{sn}^{(k)} - \nu_{sn}^c\right) \varepsilon_s^c \qquad \text{(III.B.4)}$$

Thus, the error in the boundary condition is directly proportional to the difference in Poisson's ratios between the composite and the lamina in question. The error is zero for homogeneous materials.

The free edge actually looks like Figure III.B.3. The displacement must be continuous between lamina. Thus, the displacement will vary through the thickness of a given lamina.

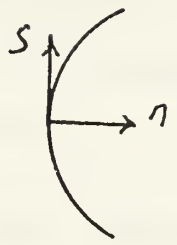

Fig. III.B.1 - Coordinate System

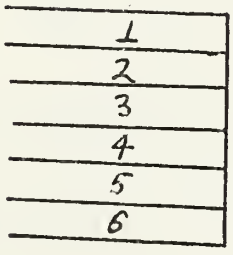

Fig. III.B.2 - Displacement for $\sigma_n^c = 0$

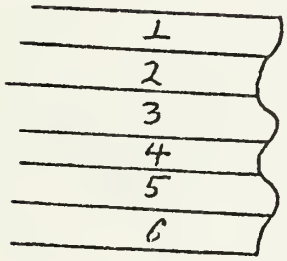

Fig. III.B.3 - Displacement for $\sigma_n^{(k)} = 0$

C. MATERIAL PROPERTIES AT A FREE BOUNDARY

It has been shown that equation III.B.2 is not the correct boundary condition for a free boundary in a laminated composite. The correct condition is

$$\sigma_n^{(k)} = 0 \quad \text{for all } k \qquad \text{(III.C.1)}$$

In order to derive the composite material properties, an additional assumption is required:

$$\varepsilon_s = \varepsilon_s^{(k)} = \varepsilon_s^c \qquad \text{(III.C.2)}$$

is constant through the thickness. Note that

$$\varepsilon_n^{(k)} = \varepsilon_n^c \qquad \text{(III.C.3)}$$

Hooke's Law for this case is

$$\sigma_s^c = E_s^c \varepsilon_s \qquad \text{(III.C.4)}$$

and

$$\sigma_s^{(k)} = E_s^{(k)} \varepsilon_s \qquad \text{(III.C.5)}$$

Recalling equation III.A.4

$$\sigma_s^c = \frac{\Sigma \sigma_s^{(k)} h^{(k)}}{\Sigma h^{(k)}}$$

or

$$E_s^c \varepsilon_s = \frac{\Sigma E_s^{(k)} \varepsilon_s h^{(k)}}{\Sigma h^{(k)}}$$

Thus

$$E_s^c = \frac{\Sigma E_s^{(k)} h^{(k)}}{\Sigma h^{(k)}} \qquad (III.C.6)$$

D. NUMERICAL RESULTS

The next step in the analysis was to find numerical values for E_s^c, Young's modulus at a free boundary and E_θ^c, Young's modulus in an arbitrary direction far from any boundaries. E_s^c may be found by use of equation III.C.6, which requires that $E_s^{(k)}$ be known for each lamina. A single lamina composite could have been made up and tested, but the data scatter inherent in the properties of glass-epoxy composites cut from different sheets would have rendered the results virtually useless for this analysis. Fortunately, this procedure was not necessary. It was possible to analytically reduce the gross laminate properties to individual lamina properties by the procedure which follows. The experimentally determined properties of the G/E/PS1-C composite are repeated here for convenience.

$E_1^c = 1.24$ MSI $\qquad \nu_{12}^c = .5$

$E_2^c = .78$ MSI $\qquad \nu_{21}^c = .31$

$G_{12}^c = .51$ MSI

The stiffness matrix may be computed from

$$C_{11} = \frac{E_1}{1-\nu_{12}\nu_{21}} \qquad C_{22} = \frac{E_2}{1-\nu_{12}\nu_{21}}$$

$$C_{12} = \frac{E_2\nu_{12}}{1-\nu_{12}\nu_{21}} \qquad C_{44} = G_{12} \qquad \text{(III.D.1)}$$

which give

$$[C] = \begin{bmatrix} 1.47 & .462 & 0 \\ .462 & .923 & 0 \\ 0 & 0 & .51 \end{bmatrix} \qquad \text{(III.D.2)}$$

The properties of the PS1-C photoelastic coating are [2]

$$E^p = .462$$

$$\nu^p = .36$$

and the stiffness matrix is

$$[C]^p = \begin{bmatrix} .528 & .190 & 0 \\ .190 & .528 & 0 \\ 0 & 0 & .169 \end{bmatrix} \qquad \text{(III.D.3)}$$

The thickness of the G/E and PS1-C portions of the composite will also be required.

$$h^c = .15$$

$$h^{c-p} = .0625$$

$$h^p = .0875$$

The thickness of the PS1-C includes the cement, which has approximately the same properties. Recalling equation III.A.7, it is possible to determine the properties of the G/E system without the photoelastic coating.

$$h^c[C]^c = h^p[C]^p + h^{c-p}[C]^{c-p} \qquad \text{(III.D.4)}$$

yields

$$[C]^{c-p} = \begin{bmatrix} 2.79 & .843 & 0 \\ .843 & 1.48 & 0 \\ 0 & 0 & .987 \end{bmatrix} \qquad \text{(III.D.5)}$$

The inverse of equations III.D.1 are [2]

$$E_1 = C_{11} - \frac{C_{12}^2}{C_{22}}$$

$$E_2 = C_{22} - \frac{C_{12}^2}{C_{11}}$$

$$\nu_{12} = \frac{C_{12}}{C_{22}} \qquad \text{(III.D.6)}$$

$$\nu_{21} = \frac{C_{12}}{C_{11}}$$

$$G_{12} = C_{44}$$

which gives the properties of the G/E system.

$$E_1^{c-p} = 2.31 \text{ MSI} \qquad \nu_{12}^{c-p} = .57$$

$$E_2^{c-p} = 1.23 \text{ MSI} \qquad \nu_{21}^{c-p} = .30$$

$$G_{12}^{c-p} = .987 \text{ MSI}$$

Recalling equation III.A.7 and noting that the thickness of each lamina in the G/E system is the same:

$$[\bar{C}]^c = \frac{\Sigma [\bar{C}]^{(k)}}{n} \qquad \text{(III.D.7)}$$

where n is the number of lamina.

Recalling that

$$[\bar{C}] = [T]^{-1}[C][T] \qquad \text{(III.D.8)}$$

it is possible to solve for [C] because all lamina are the same except for orientation! Equation III.D.8 may also be written [2]

$$\bar{C}_{11}=C_{11}\cos^4\alpha+2(C_{12}+2C_{44})\sin^2\alpha\cos^2\alpha+C_{22}\sin^4\alpha$$

$$\bar{C}_{12}=(C_{11}+C_{22}-4C_{44})\sin^2\alpha\cos^2\alpha+C_{12}(\sin^4\alpha+\cos^4\alpha)$$

$$\bar{C}_{22}=C_{11}\sin^4\alpha+2(C_{12}+2C_{44})\sin^2\alpha\cos^2\alpha+C_{22}\cos^2\alpha \qquad \text{(III.D.9)}$$

$$\bar{C}_{44}=(C_{11}+C_{22}-2C_{12}-2C_{44})\sin^2\alpha\cos^2\alpha+C_{44}(\sin^4\alpha+\cos^4\alpha)$$

Noting that the C_{ij}'s do not vary across the summation in equation III.D.7, one may proceed as follows. The orientation of the various lamina are

$$\alpha^{(1)} = \alpha^{(6)} = 0°$$

$$\alpha^{(2)} = \alpha^{(5)} = +45°$$

$$\alpha^{(3)} = \alpha^{(4)} = -45°$$

and equation III.D.7 reduces to

$$\begin{Bmatrix} C_{11} \\ C_{12} \\ C_{22} \\ C_{44} \end{Bmatrix}^{c\text{-}p} = 1/6 \begin{bmatrix} 3 & 2 & 1 & 4 \\ 1 & 4 & 1 & -4 \\ 1 & 2 & 3 & 4 \\ 1 & -2 & 1 & 2 \end{bmatrix} \begin{Bmatrix} C_{11} \\ C_{12} \\ C_{22} \\ C_{44} \end{Bmatrix} \qquad \text{(III.D.8)}$$

The inverse is

$$\begin{Bmatrix} C_{11} \\ C_{12} \\ C_{22} \\ C_{44} \end{Bmatrix} = \begin{bmatrix} 1.5 & 1 & -1.5 & 2 \\ .5 & 0 & .5 & -2 \\ -1.5 & 1 & 1.5 & 2 \\ .5 & -1 & .5 & -1 \end{bmatrix} \begin{Bmatrix} C_{11} \\ C_{12} \\ C_{22} \\ C_{44} \end{Bmatrix}^{c-p} \qquad \text{(III.D.9)}$$

which gives the stiffness matrix for a single lamina as

$$[C] = \begin{bmatrix} 4.78 & .161 & 0 \\ .161 & .852 & 0 \\ 0 & 0 & .305 \end{bmatrix} \qquad \text{(III.D.10)}$$

Applying equation III.D.6 gives the material properties of the lamina.

$\varepsilon_\ell = 4.75$ MSI $\qquad \nu_{\ell t} = .19$

$\varepsilon_t = .847$ MSI $\qquad \nu_{t\ell} = .03$

$G_{\ell t} = .305$ MSI

In order to apply equation III.C.6, $E_s^{(k)}$ must be known for each lamina. This quantity may be computed from

$$\frac{\varepsilon_\ell}{\varepsilon_s^{(k)}} = \cos^{2\theta} + \frac{\varepsilon_\ell}{\varepsilon_t} \sin^{2\theta} + 1/4\left[\frac{\varepsilon_\ell}{G_{\ell t}} - 2\nu_{\ell t}\right]\sin^2 2^{\theta}$$

or

$$\frac{1}{\varepsilon_s^{(k)}} = .211\cos^{2\theta} + 1.18\sin^{2\theta} + .8\sin^2(2^{\theta}) \qquad \text{(III.D.11)}$$

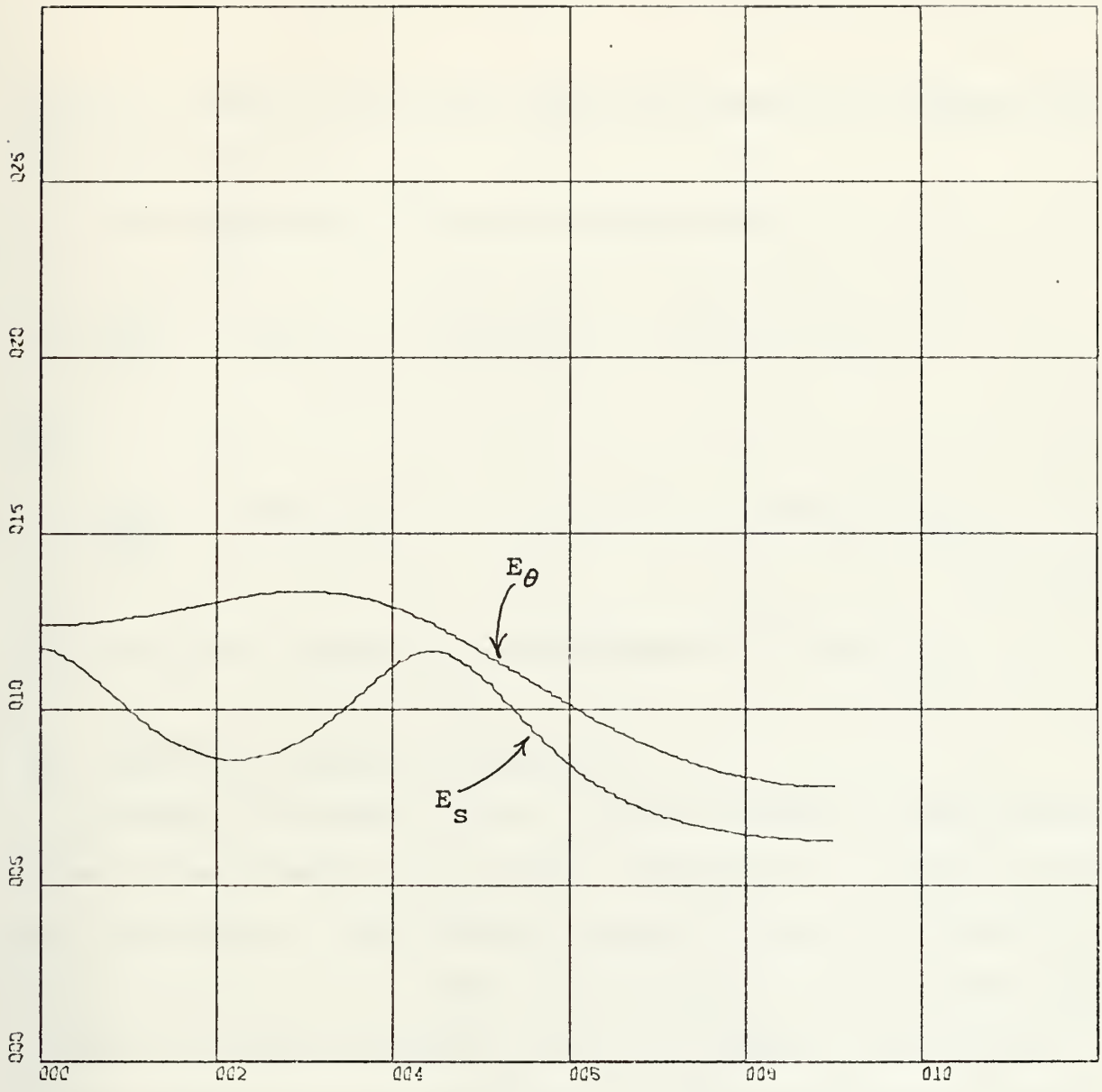

X-SCALE=2.00E+01 UNITS INCH.
Y-SCALE=5.00E-01 UNITS INCH.

FIGURE III.D.1 - Young's Modulus Curves

SABA0072

$E_s^{(k)}$ is computed for each lamina and then E_s^c is computed for equation III.C.6.

For comparison, E^c may be computed from

$$\frac{1.24}{E_\theta^c} = \cos^2\theta + 1.59 \sin^2\theta + .358 \sin^2(2\theta)$$

or

$$\frac{1}{E_\theta^c} = .806 \cos^2\theta + 1.28 \sin^2\theta + .289 \sin^2(2\theta) \qquad \text{(III.D.12)}$$

E_θ^c and E_s^c are plotted as a function of θ in Figure III.D.1.

E. EFFECT ON STRESS CONCENTRATION

As seen in Figure III.D.1, Young's modulus in the y direction at the boundary is 1.17 MSI compared to 1.24 MSI far from all boundaries. The variation along the X-axis is something like Figure III.E.1. Thus, the material at the boundaries is less stiff than the material near the center of the plate. Now, suppose that the theoretical stress concentration variation for constant material properties is given by curve A in Figure III.E.2. The variation in material properties described by Figure III.E.1 would tend to reduce the stress concentration near the boundaries, because the material is less stiff in these areas (Curve B). This effect is shown clearly at the boundaries of the plates in Figures II.D.2-5. Thus, the lower stiffness near a free boundary in a laminated composite

requires that the stress concentration factor be smaller than that given by homogeneous orthotropic theory.

The effect described above can also be shown to vary with the hole size. The modulus of elasticity of the laminated composite is lowest at the free boundary and increases to a steady value at a finite distance from the boundary as shown in Figure III.E.1. The actual function will depend on component materials and layup of composite, but will depend only on the X distance from the free edge for a particular composite:

$$E_1 = E_1 (X) \qquad \text{(III.E.1)}$$

The stress concentration along the X-axis, however, is a function of the number of hole radii away from the boundary:

$$K = K(X/r) \qquad \text{(III.E.2)}$$

Thus, in terms of the normalized distance, X/r, a plate with a small hole is affected more by the difference in stiffness than a plate with a large hole. Therefore, the smaller the hole, the smaller the stress concentration factor, even in an infinite plate or plates with a constant hole-size-to-plate-width ratio.

If Young's modulus in Figure III.E.1 is assumed to vary like Curve B, rather than Curve A, one has the problem of stress concentration around holes which are strengthened by elastic rings. This problem has been solved by Savin [4] who describes similar results. The theoretical stress concentration for infinite copper plates with holes strengthened by

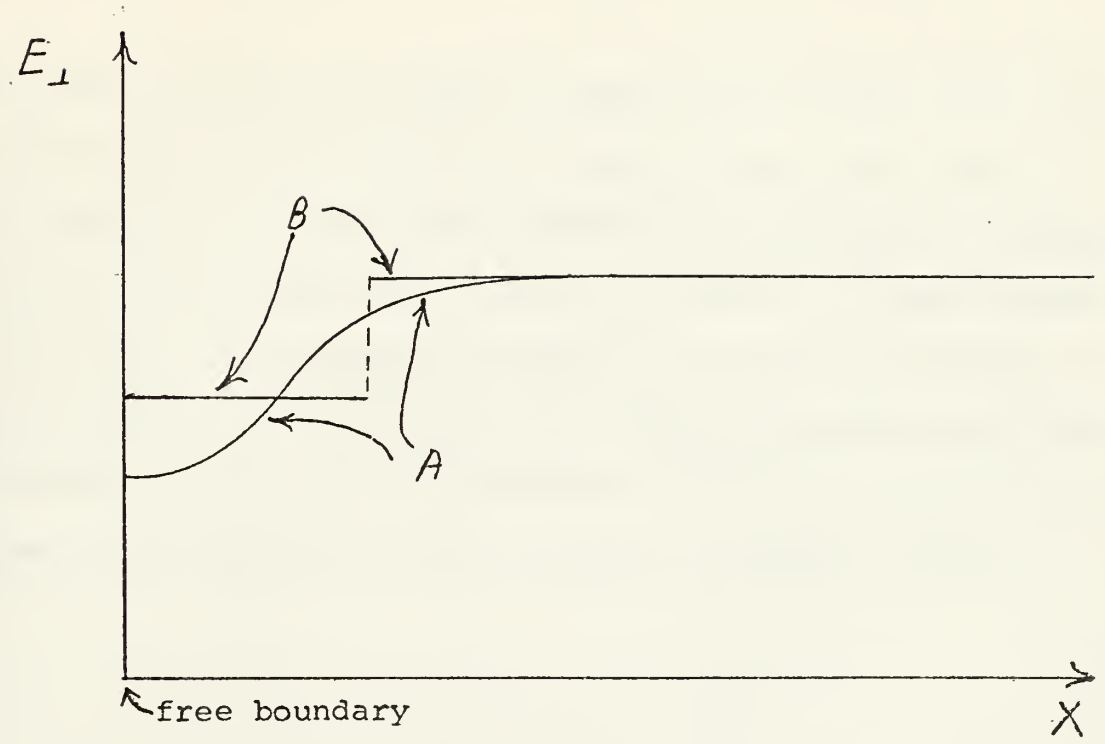

FIGURE III.E.1 - E near a free boundary

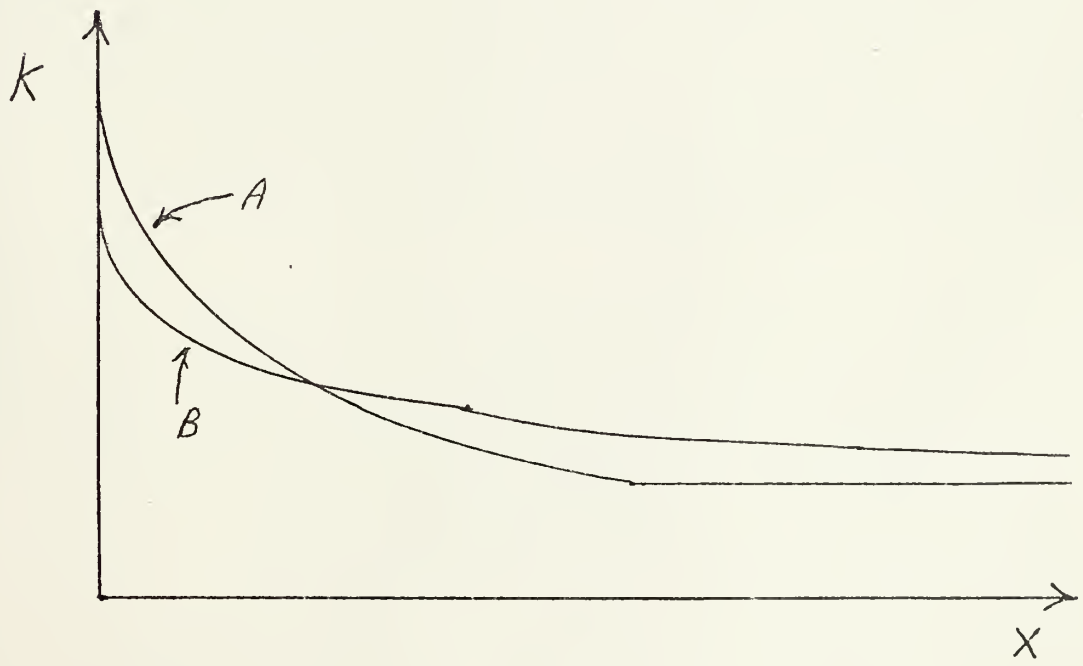

FIGURE III.E.2 - Inhomogeneous effects on k

steel rings of various widths is presented by Savin and this set of curves is very similar to Figure II.E.5, the experimental results for plates with different size holes. Consider a series of such rings, one inside the other. A large number of thin rings with appropriate material properties could be used to produce the variation in stiffness described by Curve A of Figure III.E.1. It is suggested that this approach be further investigated in order to obtain numerical results.

IV. CONCLUSION

The first objective of this research was to show experimentally that the homogeneous orthotropic solution for stress concentration around a circular hole is not accurate for laminated fibrous composites. Referring to Figure III.E.5, the following stress concentration factors are obtained:

TABLE IV.1

Theory	3.15
Plate 1203 (r = .25")	3.07
Plate 1205 (r = .125")	2.45
Plate 1206 (r = .0625")	2.01

Obviously, the theory is not accurate. The second objective was to determine whether hole size has an effect on the stress concentration in an infinite plate. Referring to Table IV.1 again, it is obvious that the stress concentration factor decreases with hole size.

The third objective was to analyze the effects of inhomogeneity on stress concentration. It was found that to enforce the boundary condition at a free edge required the modification of the gross laminate properties near the edge. The lower stiffness obtained analytically required that the stress concentration factor be lower than that predicted by homogeneous orthotropic theory. Furthermore, it was shown that the stress concentration factor varies with hole size

because the modified material properties affect a larger normalized area for smaller holes.

APPENDIX A: EXPERIMENTAL DATA

A-1 MATERIAL PROPERTIES TEST DATA

MATERIAL PROPERTIES TEST 9 APR 75

PLATE # 1200

OF RUNS: 4 AREA 0.150 F = 40.248

P	SIGMA	NN	NO	DELNN	DELNO	EPSY	EPSX	NU
0	0	1.1	-2.7					
100	666	22.9	20.2	21.8	22.9	505	-372	.737
200	1333	43.0	46.6	41.9	49.3	1239	-396	.307
300	2000	62.5	66.6	61.4	69.3	1712	-758	.443
400	2666	78.7	84.4	77.6	87.1	2135	-988	.463
500	3333	94.5	106.1	93.4	108.8	2809	-949	.338
0	0	0.4	-2.7					
100	666	22.6	19.7	22.2	22.4	458	-434	.948
200	1333	41.5	43.2	41.1	45.9	1116	-537	.481
300	2000	61.4	64.9	61.0	67.6	1626	-829	.510
400	2666	79.8	86.6	79.4	89.3	2195	-1000	.455
500	3333	96.7	107.5	96.2	110.2	2777	-1098	.395
0	0	-1.4	-3.0					
100	666	20.9	21.0	22.3	24.0	551	-346	.628
200	1333	40.2	42.0	41.6	45.0	1042	-631	.606
300	2000	61.1	65.4	62.5	68.4	1613	-901	.559
400	2666	81.2	90.4	82.6	93.4	2314	-1010	.436
500	3333	98.1	106.4	99.5	109.4	2600	-1404	.540
0	0	2.0	1.7					
100	666	19.6	10.2	17.6	8.5	-195	-903	****
200	1333	42.5	45.0	40.5	43.3	984	-645	.655
300	2000	60.8	66.5	58.8	64.8	1545	-821	.531
400	2666	80.1	87.6	78.1	85.9	2042	-1100	.539
500	3333	99.1	109.3	97.1	107.6	2587	-1320	.510

MATERIAL PROPERTIES TEST 6 MAY 75

PLATE # 1210

OF RUNS: 4 AREA 0.150 F = 40.248

P	SIGMA	NN	NO	DELNN	DELNO	EPSY	EPSX	NU
0	0	-0.3	-0.8					
100	666	17.1	19.4	17.4	20.2	519	-181	.349
200	1333	33.0	38.3	33.3	39.1	1020	-319	.313
300	2000	49.0	57.3	49.3	58.1	1523	-460	.302
400	2666	66.0	77.2	66.3	78.0	2040	-627	.307
500	3333	81.7	94.3	82.0	95.1	2441	-859	.352
0	0	1.4	-3.5					
100	666	18.2	20.4	16.8	23.9	766	90	****
200	1333	34.1	40.5	32.7	44.0	1340	24	****
300	2000	51.0	60.4	49.6	63.9	1861	-134	.072
400	2666	66.0	81.0	64.6	84.5	2501	-98	.039
500	3333	81.6	98.2	80.2	101.7	2911	-315	.108
0	0	-1.3	-1.0					
100	666	20.8	23.5	22.1	24.5	589	-299	.508
200	1333	38.4	39.4	39.7	40.4	841	-756	.899
300	2000	53.4	56.5	54.7	57.5	1259	-931	.734
400	2666	71.0	77.0	72.3	78.0	1799	-1110	.617
500	3333	83.8	97.0	85.1	98.0	2491	-933	.375
0	0	-1.3	-1.0					
100	666	24.5	19.5	25.8	20.5	199	-839	****
200	1333	37.7	41.0	39.0	42.0	965	-603	.625
300	2000	55.3	58.7	56.6	59.7	1326	-951	.717
400	2666	71.0	80.1	72.3	81.1	1986	-923	.465
500	3333	87.0	95.1	88.3	96.1	2247	-1306	.581

MATERIAL PROPERTIES TEST 6 MAY 75

PLATE # 1220

OF RUNS: 4 AREA 0.150 F = 40.248

P	SIGMA	NN	NO	DELNN	DELNO	EPSY	EPSX	NU
0	0	1.0	-2.0					
100	666	29.8	28.2	28.8	30.2	664	-495	.745
200	1333	55.9	65.2	54.9	67.2	1847	-362	.196
300	2000	82.7	94.6	81.7	96.6	2543	-744	.292
400	2666	109.0	127.2	108.0	129.2	3453	-893	.259
0	0	2.6	1.0					
100	666	31.0	29.8	28.4	28.8	595	-547	.919
200	1333	55.4	66.4	52.8	65.4	1823	-301	.165
300	2000	83.8	96.8	81.2	95.8	2515	-752	.299
400	2666	110.0	130.2	107.4	129.2	3477	-845	.243
0	0	3.4	-1.2					
100	666	32.5	31.7	29.1	32.9	815	-356	.437
200	1333	59.0	64.6	55.6	65.8	1734	-503	.290
300	2000	86.7	98.3	83.3	99.5	2654	-698	.263
400	2666	112.8	128.6	109.4	129.8	3433	-969	.282
0	0	2.6	-1.6					
100	666	33.5	28.2	30.9	29.8	553	-688	****
200	1333	56.4	64.5	53.8	66.1	1825	-340	.186
300	2000	86.6	96.0	84.0	97.6	2511	-869	.346
400	2666	112.7	129.0	110.1	130.6	3453	-978	.283

A-2 STRESS CONCENTRATION TEST DATA

STRESS CONCENTRATION DATA 29 MAY 75

PLATE # 1203 X-AXIS

OF RUNS: 2 LOAD 800.0 F= 36.596

X/R	TNN	TNO	NN	NO	EPSY	EPSX	K	A
FF	-2.0	-6.5	43.5	43.8	1096	-569	1.00	0.52
1.0	-8.0	-6.5	120.4	******	3455	******	3.15	******
1.3	-2.0	-6.5	75.0	75.4	1677	-1139	1.53	0.68
1.5	-2.0	-6.5	55.5	60.5	1573	-530	1.44	0.34
1.8	-2.0	-6.5	45.6	49.6	1337	-404	1.22	0.30
2.0	-2.0	-6.5	45.6	46.4	1161	-580	1.06	0.50
2.5	-2.0	-6.5	45.6	46.4	1161	-580	1.06	0.50
3.0	-2.0	-6.5	45.6	46.4	1161	-580	1.06	0.50
4.0	-2.0	-6.5	45.6	46.4	1161	-580	1.06	0.50
5.0	-2.0	-6.5	45.6	46.4	1161	-580	1.06	0.50
6.0	-8.0	-6.5	30.7	******	1041	******	0.95	******
FF	-2.0	-6.5	43.5	43.8	1096	-569	1.00	0.52
1.0	-5.8	-6.5	113.2	******	3202	******	2.92	******
1.3	-2.0	-6.5	76.7	87.0	2252	-627	2.05	0.28
1.5	-2.0	-6.5	56.8	73.1	2217	65	2.02	-0.03
1.8	-2.0	-6.5	47.3	57.7	1720	-84	1.57	0.05
2.0	-2.0	-6.5	47.3	50.0	1297	-506	1.18	0.39
2.5	-2.0	-6.5	47.3	50.0	1297	-506	1.18	0.39
3.0	-2.0	-6.5	47.3	50.0	1297	-506	1.18	0.39
4.0	-2.0	-6.5	47.3	50.0	1297	-506	1.18	0.39
5.0	-2.0	-6.5	47.3	50.0	1297	-506	1.18	0.39
6.0	-8.0	-6.5	35.4	******	1167	******	1.06	******

STRESS CONCENTRATION DATA 28 MAY 75

PLATE # 1205 X-AXIS

OF RUNS: 2 LOAD 400.0 F= 40.248

X/R	TNN	TNO	NN	NO	EPSY	EPSX	K	A
FF	-0.5	-5.0	51.7	53.4	1424	-676	1.00	0.47
1.0	-2.5	-5.0	117.5	******	3551	******	2.49	******
1.5	-0.5	-5.0	63.2	82.1	2694	130	1.89	-0.05
2.0	-0.5	-5.0	49.9	51.7	1394	-633	0.98	0.45
2.5	-0.5	-5.0	49.9	51.7	1394	-633	0.98	0.45
3.0	-0.5	-5.0	49.9	51.7	1394	-633	0.98	0.45
4.0	-0.5	-5.0	49.9	51.7	1394	-633	0.98	0.45
5.0	-0.5	-5.0	49.9	51.7	1394	-633	0.98	0.45
6.0	-6.5	-5.0	36.1	******	1260	******	0.88	******
FF	-0.5	-5.0	51.7	53.4	1424	-676	1.00	0.47
1.0	-5.2	-5.0	111.0	******	3438	******	2.41	******
1.5	-5.2	-5.0	50.8	76.0	2636	382	1.85	-0.14
2.0	-5.2	-5.0	49.1	51.0	1195	-990	0.84	0.83
2.5	-5.2	-5.0	49.1	51.0	1195	-990	0.84	0.83
3.0	-5.2	-5.0	49.1	51.0	1195	-990	0.84	0.83
4.0	-5.2	-5.0	49.1	51.0	1195	-990	0.84	0.83
5.0	-5.2	-5.0	49.1	51.0	1195	-990	0.84	0.83
6.0	-2.6	-5.0	40.2	******	1266	******	0.89	******

STRESS CONCENTRATION DATA 29 MAY 75

PLATE # 1206 X-AXIS

OF RUNS: 2 LOAD 200.0 F= 36.596

X/R	TNN	TNC	NN	NO	EPSY	EPSX	K	A
FF	-1.0	-5.5	55.6	61.2	1590	-481	1.00	0.30
1.0	-8.0	-5.5	109.0	******	3148	******	1.98	******
2.0	-1.0	-5.5	46.6	67.5	2265	523	1.42	-0.23
3.0	-1.0	-5.5	46.6	57.4	1710	-31	1.08	0.02
4.0	-1.0	-5.5	46.6	57.4	1710	-31	1.08	0.02
5.0	-1.0	-5.5	46.6	57.4	1710	-31	1.08	0.02
6.0	-5.8	-5.5	40.1	******	1235	******	0.78	******
FF	-1.0	-5.5	55.6	61.2	1590	-481	1.00	0.30
1.0	-8.0	-5.5	112.0	******	3229	******	2.03	******
2.0	-1.0	-5.5	52.7	64.1	1855	-109	1.17	0.06
3.0	-1.0	-5.5	52.7	53.5	1273	+691	0.80	0.54
4.0	-1.0	-5.5	52.7	53.5	1273	-691	0.80	0.54
5.0	-1.0	-5.5	52.7	53.5	1273	-691	0.80	0.54
6.0	-5.8	-5.5	41.6	******	1275	******	0.80	******

STRESS CONCENTRATION DATA 29 MAY 75

PLATE # 1203 Y-AXIS

OF RUNS: 2 LOAD 800.0 F= 36.596

Y/R	TNN	TNO	NN	NO	EPSX	EPSY	K	A
FF	-2.0	-6.5	43.5	43.8	1096	-569	1.00	0.52
1.0	15.5	-6.5	68.7	******	-1431	******	-1.31	******
1.3	-2.0	-6.5	20.4	7.0	-898	-78	-0.82	-11.51
1.5	-2.0	-6.5	14.3	4.0	-616	-20	-0.56	-30.80
1.8	-2.0	-6.5	10.2	9.3	-25	420	-0.02	0.06
2.0	-2.0	-6.5	16.7	14.5	-215	468	-0.20	0.46
2.5	-2.0	-6.5	26.4	22.0	-514	525	-0.47	0.98
3.0	-2.0	-6.5	30.1	30.6	-312	861	-0.28	0.36
4.0	-2.0	-6.5	38.0	33.5	-731	731	-0.67	1.00
5.0	-2.0	-6.5	40.0	39.1	-570	966	-0.52	0.59
6.0	-2.0	-6.5	40.0	39.1	-570	966	-0.52	0.59
FF	-2.0	-6.5	43.5	43.8	1096	-569	1.00	0.52
1.0	14.0	-6.5	70.5	******	-1520	******	-1.39	******
1.3	-2.0	-6.5	24.3	13.4	-832	129	-0.76	6.45
1.5	-2.0	-6.5	14.4	2.5	-706	-106	-0.64	-6.66
1.8	-2.0	-6.5	14.6	6.4	-506	100	-0.46	5.06
2.0	-2.0	-6.5	22.1	14.0	-638	243	-0.58	2.63
2.5	-2.0	-6.5	26.9	22.5	-523	534	-0.48	0.98
3.0	-2.0	-6.5	33.2	32.5	-435	852	-0.40	0.51
4.0	-2.0	-6.5	38.2	38.3	-483	988	-0.44	0.49
5.0	-2.0	-6.5	42.6	41.5	-629	1002	-0.57	0.63
6.0	-2.0	-6.5	44.5	43.5	-658	1042	-0.60	0.63

STRESS CONCENTRATION DATA 28 MAY 75

PLATE # 1205 Y-AXIS

OF RUNS: 2 LOAD 400.0 F= 40.248

Y/R	TNN	TNO	NN	NO	EPSX	EPSY	K	A
FF	-0.5	-5.0	51.7	53.4	1424	-676	1.00	0.47
1.0	-5.8	-5.0	63.4	******	-2047	******	-1.44	******
1.5	-0.5	-5.0	2.0	2.1	227	328	0.16	-0.69
2.0	-0.5	-5.0	18.5	22.4	124	889	0.09	-0.14
2.5	-0.5	-5.0	31.3	28.5	-537	742	-0.38	0.72
3.0	-0.5	-5.0	35.2	34.5	-489	947	-0.34	0.52
4.0	-0.5	-5.0	38.0	41.5	-291	1257	-0.20	0.23
5.0	-0.5	-5.0	45.0	43.3	-746	1084	-0.52	0.69
6.0	-0.5	-5.0	46.7	46.2	-708	1191	-0.50	0.59
FF	-0.5	-5.0	51.7	53.4	1424	-676	1.00	0.47
1.0	-0.8	-5.0	65.5	******	-1962	******	-1.38	******
1.5	-0.5	-5.0	4.6	4.7	175	380	0.12	-0.46
2.0	-0.5	-5.0	18.0	22.4	165	909	0.12	-0.18
2.5	-0.5	-5.0	29.8	28.5	-416	802	-0.29	0.52
3.0	-0.5	-5.0	35.7	34.5	-529	927	-0.37	0.57
4.0	-0.5	-5.0	40.3	41.5	-476	1165	-0.33	0.41
5.0	-0.5	-5.0	44.2	43.3	-682	1116	-0.48	0.61
6.0	-0.5	-5.0	46.4	46.2	-684	1203	-0.48	0.57

STRESS CONCENTRATION DATA 29 MAY 7

PLATE # 1206 Y-AXIS

OF RUNS: 2 LOAD 200.0 F= 36.596

Y/R	TNN	TNO	NN	NO	EPSX	EPSY	K	A
FF	-1.0	-5.5	55.6	61.2	1590	-481	1.00	0.30
1.0	11.2	-5.5	55.6	******	-1194	******	-0.75	******
2.0	-1.0	-5.5	19.8	44.7	1233	1994	0.78	-0.62
3.0	-1.0	-5.5	33.5	38.0	-137	1125	-0.09	0.12
4.0	-1.0	-5.5	43.0	43.1	-552	1057	-0.35	0.52
5.0	-1.0	-5.5	46.0	49.0	-448	1271	-0.28	0.35
6.0	-1.0	-5.5	48.0	49.0	-594	1198	-0.37	0.50
FF	-1.0	-5.5	55.6	61.2	1590	-481	1.00	0.30
1.0	11.2	-5.5	55.8	******	-1200	******	-0.75	******
2.0	-1.0	-5.5	27.7	34.7	106	1156	0.07	-0.09
3.0	-1.0	-5.5	36.8	37.5	-406	977	-0.26	0.42
4.0	-1.0	-5.5	45.1	44.5	-629	1057	-0.40	0.60
5.0	-1.0	-5.5	46.6	44.4	-744	997	-0.47	0.75
6.0	-1.0	-5.5	49.0	47.0	-777	1052	-0.49	0.74

APPENDIX B: COMPUTER PROGRAMS

B-1 MATERIAL PROPERTIES PROGRAM

```
      EQUIVALENCE (TITLE,RTB(5))
      REAL*4 TITLE(15),STRA(15),NN,NO,NU,EPSY(30),SIGMA(30)
      INTEGER*4 P,EPSX
      INTEGER*4 ITB(12)/12*0/
      REAL*4 RTB(28)/28*0.0/
      ITB(1)=1
      ITB(2)=0
      ITB(3)=6
      ITB(4)=6
      ITB(7)=1
      ITB(10)=2
      ITB(11)=1
C          INITIAL ALPHANUMERIC DATA
      READ(5,100) STRA
  100 FORMAT(15A4)
      WRITE(6,110) STRA
  110 FORMAT('1',15A4)
      READ(5,100) TITLE
      WRITE(6,120) TITLE
  120 FORMAT('0',15A4)
      READ(5,130) K1,A,F
  130 FORMAT(10X,I2,8X,F10.5,4X,F10.5)
      WRITE(6,140) K1,A,F
  140 FORMAT('0# OF RUNS:',I2,'   AREA ',F6.3,'      F = ',F7
     .3
      DO 30 I=1,10
      READ(5,100) STRA
   30 WRITE(6,150) STRA
      READ(5,100) STRA
      WRITE(6,120) STRA
      READ(5,100) STRA
      WRITE(6,150) STRA
  150 FORMAT(' ',15A4)
      DO 20 J=1,K1
C
C
      READ(5,155) K2
  155 FORMAT(54X,I2)
      READ(5,100) STRA
C          TARE VALUES
      READ(5,160) P,TNN,TNO
  160 FORMAT(I10,2F10.4)
      ISIGMA=P/A
      WRITE(6,170) P,ISIGMA,TNN,TNO
  170 FORMAT('0',I4,1X,I5,2(1X,F6.1))
C          DATA REDUCTION
C
      DO 10 I=1,K2
C
      READ(5,160) P,NN,NO
      ISIGMA=P/A
      SIGMA(I)=FLOAT(ISIGMA)
      DELNN=NN-TNN
      DELNO=NO-TNO
      IEPSY=F*(1.5*DELNO-DELNN)
      EPSY(I)=FLOAT(IEPSY)
      EPSX=F*(1.5*DELNO-2.*DELNN)
      NU=-EPSX/EPSY(I)
   10 WRITE(6,180) P,ISIGMA,NN,NO,DELNN,DELNO,IEPSY,EPSX,NU
  180 FORMAT(' ',I4,1X,I5,4(1X,F6.1),2(2X,I6),2X,F4.3)
      IF(J.EQ.K1) WRITE(6,110)
C          PLOT STRESS-STRAIN CURVE
      IF(J.GT.1) ITB(1)=2
```

```
      IF(J.EQ.K1) ITB(1)=3
      ITB(2)=ITB(2)+1
      IF(ITB(2).EQ.5) ITB(2)=1
      CALL DRAWP(K2,EPSY,SIGMA,ITB,RTB)
   20 CONTINUE
      STOP
      END
```

B-2 STRESS CONCENTRATION PROGRAM

```
      EQUIVALENCE (TITLE,RTB(5))
      REAL*4 TITLE(15),STRA(15),NN,NO,K(30),X(30),A(30),KF
      INTEGER*4 EPSX,FEPSY
      INTEGER*4 ITB(12)/12*0/
      REAL*4 RTB(28)/28*0.0/
      ITB(1)=1
      ITB(2)=3
      ITB(3)=6
      ITB(4)=6
      ITB(7)=1
      ITB(10)=2
      ITB(11)=1
      DO 1 ICOUNT=1,3
C          INITIAL ALPHANUMERIC DATA
      READ(5,100) STRA
  100 FORMAT(15A4)
      WRITE(6,110) STRA
  110 FORMAT('1',15A4)
      READ(5,100) TITLE
      WRITE(6,120) TITLE
  120 FORMAT('0',15A4)
      READ(5,130) K1,P,F
  130 FORMAT(10X,I2,8X,F10.5,4X,F10.5)
      WRITE(6,140) K1,P,F
  140 FORMAT('0# OF RUNS:',I2,'   LOAD ',F6.1,'      F= ',F7.
     3)
      DO 30 I=1,10
      READ(5,100) STRA
   30 WRITE(6,150) STRA
      READ(5,100) STRA
      WRITE(6,120) STRA
      READ(5,100) STRA
      WRITE(6,150) STRA
  150 FORMAT(' ',15A4)
      DO 20 J=1,K1
C
C
      READ(5,155) K2
  155 FORMAT(54X,I2)
      READ(5,100) STRA
C          FAR FIELD VALUES
      READ(5,160) TNN,TNO,NN,NO
  160 FORMAT(10X,4F10.4)
      DELNN=NN-TNN
      DELNO=NO-TNO
      FEPSY=F*(1.5*DELNO-DELNN)
      EPSX=F*(1.5*DELNO-2.*DELNN)
      KF=1.0
      AF=-EPSX/FLOAT(FEPSY)
      WRITE(6,170) TNN,TNO,NN,NO,FEPSY,EPSX,KF,AF
  170 FORMAT('0FF  ',2(F5.1,1X),2(F6.1,1X),2(I6,1X),F5.2,1X,
     F6.2)
C          DATA REDUCTION
      DO 10 I=1,K2
      READ(5,165) X(I),TNN,TNO,NN,NO
  165 FORMAT(5F10.4)
      DELNN=NN-TNN
      DELNO=NO-TNO
      IEPSY=F*(1.5*DELNO-DELNN)
      EPSX=F*(1.5*DELNO-2.*DELNN)
    6 K(I)=IEPSY/FLOAT(FEPSY)
      A(I)=-EPSX/FLOAT(IEPSY)
      IF(NO.NE.0.0) GO TO 10
      IEPSY=F*DELNN/1.36
      NO=10**8
      EPSX=10**8
      K(I)=IEPSY/FLOAT(FEPSY)
```

```
      A(I)=10**8
   10 WRITE(6,180) X(I),TNN,TNO,NN,NO,IEPSY,EPSX,K(I),A(I)
  180 FORMAT(' ',F3.1,1X,2(F5.1,1X),2(F6.1,1X),2(I6,1X),F5.2
     ,1X,F6.2)
      IF(J.EQ.K1) WRITE(6,110)
C          PLOT STRESS-STRAIN CURVE
      IF(J.GT.1) ITB(1)=2
      IF(ICOUNT.NE.3) GO TO 2
      IF(J.EQ.K1) ITB(1)=3
    2 CONTINUE
      CALL DRAWP(K2,X,K,ITB,RTB)
   20 CONTINUE
      ITB(2)=ITB(2)+1
      IF(ITB(2).EQ.6) ITB(2)=1
    1 CONTINUE
      STOP
      END
```

LIST OF REFERENCES

1. Advanced Composites Design Guide, Vol. IV, Rockwell International Corporation, 1973.

2. Calcote, L. R., The Analysis of Laminated Composite Structures, Van Nostrand Reinhold Company, 1969.

3. Lekhnitskii, S. G., Aristropic Plates, Gordon and Breach Science Publishers, 1968.

4. Savin, G. N., Stress Concentration Around Holes, Pergammon Press, 1961.

INITIAL DISTRIBUTION LIST

		No. Copies
1.	Defense Documentation Center Cameron Station Alexandria, Virginia 22314	2
2.	Library, Code 0212 Naval Postgraduate School Monterey, California 93940	2
3.	Dean of Research, Code 023 Naval Postgraduate School Monterey, California 93940	1
4.	Department Chairman, Code 57 Department of Aeronautics Naval Postgraduate School Monterey, California 93940	2
5.	Dr. M. H. Bank, Code 57Bt Department of Aeronautics Naval Postgraduate School Monterey, California 93940	10
6.	Dr. George C. Chang Aerospace Engineering Department United States Naval Academy Annapolis, Maryland 21402	1
7.	Dr. Al Someroff NAIR-320B Naval Air Systems Command Headquarters Washington, D. C. 20361	1
8.	ENS David L. Saba 12426 Largo Drive Savannah, Georgia 31406	1

161248

Thesis
S115 Saba
c.1 Stress concentration
around holes in laminated
fibrous composites.